Next Generation Anodes for Lithium-Ion Batteries

Third Quarter Progress Report 2019

Jack Vaughey
Argonne National Laboratory
9700 South Cass Avenue
Lemont, IL 60439
Phone: (630) 252-8885
E-mail: vaughey@anl.gov

Brian Cunningham, DOE-EERE-VTO Program Manager
Hybrid Electric Systems, Battery R&D
Phone: (202) 586-8055
E-mail: brian.cunningham@ee.doe.gov

Table of Contents

Silicon Deep Dive Overview

Project Introduction

Silicon has received significant attention as an alternative to the graphitic carbon negative electrodes presently used in a lithium-ion battery due to its high capacity and availability. Compared to graphitic carbons, elemental silicon's capacity is nearly an order of magnitude higher (~3600 mAh/g silicon vs 372 mAh/g Graphite). However, several problems have been identified that limit its utility including a large crystallographic expansion (~320%) upon full lithiation, slow lithium diffusion, and high reactivity at high states of charge. Together these physical properties result in particle cracking, particle isolation, electrolyte reactivity, and electrode delamination issues. These chemical reactivity and volume changes are manifested in SEI stability (calendar and life studies) and cycling efficiency issues for the cell. Because of the technological advances possible if a silicon anode can be designed and proven, researchers in multiple disciplines have pushed to understand these physical issues and advance the field and create a viable silicon-based electrode.

Next Generation Anodes for Lithium-Ion Batteries, also referred to as the silicon Deep Dive Program, is a consortium of five National Laboratories assembled to tackle the barriers associated with development of an advanced lithium-ion negative electrode based upon silicon as the active material. This research program has several goals including (1) evaluating promising silicon materials that can be either developed by a team member or obtained in quantities sufficient for electrode preparation by the consortiums facilities, (2) developing a composite silicon-Gr electrode that meets BatPac specifications, and (3) executing full cell development strategies that leverage DOE-EERE-VTO investments in electrode materials and characterization. The primary objective of this program is to understand and eliminate the barriers to implementation of a silicon based anode in a lithium-ion cell. The Five National Laboratories (ANL, NREL, LBNL, ORNL, and SNL) involved are focused on a single program with continuous interaction, clear protocols for analysis, and targets for developing both an understanding and a cell chemistry associated with advance negative electrodes for lithium-ion cells. This undertaking is a full electrode/full cell chemistry project with efforts directed at understanding and developing the chemistry needed for advancing silicon-based anodes operating in full cells. Materials development efforts include active material development, binder synthesis, coatings, safety, and electrolyte additives. Efforts include diagnostic research from all partners, which span a wide range of electrochemical, chemical and structural characterization of the system across length- and time-scales. Specialized characterization techniques developed with DOE-EERE-VTO funding, include neutrons, MAS-NMR, optical, and X-ray techniques being employed to understand operation and failure mechanisms in silicon-based anodes. In addition, several strategies to mitigate lithium loss are being assessed. The project is managed as a single team effort spanning the Labs, with consensus decisions driving research directions and toward development of a functioning stable silicon-based electrode.

The silicon Deep Dive project seeks to identify the limiting factors of silicon-based electrodes that need to be overcome to produce a viable functioning LIB electrode and full cell. The issues include understanding and controlling silicon surface chemistry, lithium loss due to side reactions, active material interactions, and the role of electrolyte stability. The goal of the project is utilize our understanding of silicon and silicide reactivity, electrode formulation, and binder and electrolyte formulations, to design a functioning silicon-based electrode for a lithium-ion cell that meets DOE-EERE goals. Combined with the SEISta's efforts focused on interfacial reactivity, composition, and stability, key variables can be isolated and studied to improve the performance of a silicon-based cell. This key interaction is maintained and accomplished through joint meetings, face to face discussions, and extensive collaborations between the teams.

FY19 Deep Dive Goals:

Q1 Demonstrate improved cycling efficiency of a silicon-based electrode that incorporates either an inorganic or organic surface modification compared to uncoated silicon baseline

Q2 Exhibit a binder designed to strongly interact with the silicon particle surface that shows enhanced cycling stability versus an LiPAA baseline.

Q3 Demonstrate that controlling lithium inventory in a full cell can extend cycle life of a silicon-based electrode by at least 10%.

Q4 Construct and evaluate cells based on optimizing lithium inventory, binder, electrolyte formulation, and testing protocol to achieve a 300 Wh/kg cell design.

Approach

Oak Ridge National Laboratory (ORNL), National Renewable Energy Laboratory (NREL), Pacific Northwest National Laboratory (PNNL), Lawrence Berkeley National Laboratory (LBNL), and Argonne National Laboratory (ANL) have teamed together to form an integrated program. Technical targets have been developed and regular communications have been established. Throughout the program, there is a planned focus on understanding, insights into, and advancement of, silicon-based materials, electrodes, and cells. All anode advancements will be verified based on life and performance of full cells. Toward that end, baseline silicon-based materials, electrodes, and cells have been adopted, along with full cell testing protocols.

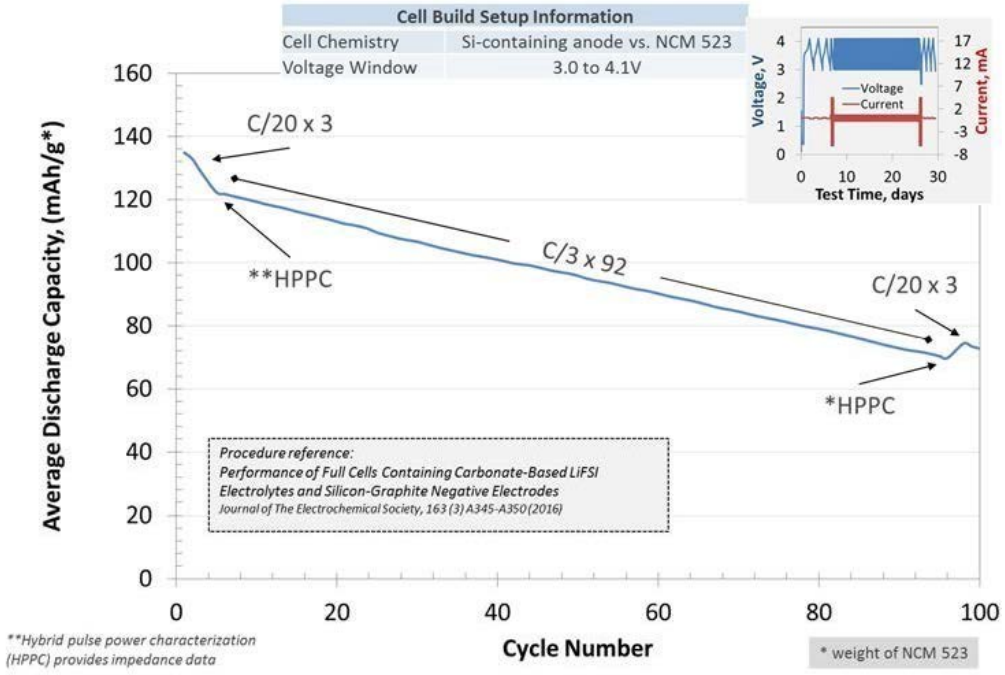

Figure 1. Full cell testing protocol.

In examining improvements, changes to the baseline cell technology will be minimized. As an example, silicon active material coating improvements will be verified on baseline silicon materials in electrodes fabricated by the battery research facilities. All other components in the prototype cells (i.e. positive electrode, separator, and electrolyte) will be from the baseline technology. While there are many testing protocols that can be utilized to

benchmark the baseline technology, this program has adopted a testing protocol from the literature that has worked well for lithium-ion cells with silicon containing anodes. Shown pictorially in **Figure** 1 the test starts with three slow (C/20) formation cycles, an HPPC cycle, and then the C/3 aging cycles. The test ends with another HPPC cycle and three more slow (C/20) cycles. All constant current cycling is symmetric between charge and discharge rates. The tests are run at 30°C. If there is little or no aging in the first 100 cycles, the protocol can be repeated. This protocol effectively examines capacity, impedance, and aging effects in about a month's worth of testing. As the program matures, materials developments will be incorporated into baseline silicon-based materials, electrodes, and cells. Scale-up of materials, incorporation of materials advancements into electrodes and prototype cells, and characterization and testing of cells, as well as evaluation of safety and abuse tolerance are part of a wide range of integrated studies supported by battery research facilities at the National Labs working closely with the program. These research facilities include the Battery Abuse Testing Laboratory (BATLab), the Battery Manufacturing Facility (BMF), the Cell Analysis, Modeling, and Prototyping (CAMP) facility, the Materials Engineering Research Facility (MERF), and the Post-Test Facility (PTF). At the present time the baseline silicon is from Paraclete Energy (Chelsea, MI).

The fundamental understanding of silicon-based electrode active materials is based on extensive electrochemical and analytical diagnostic studies on components, electrodes, and cells conducted within the program. This effort contains in-situ and ex-situ studies on full and specialty cells, including reference electrode cells. Overall, the diagnostic studies are intended to help establish structure-composition-property relationships, including lithium-reactivity at the silicon surface and bulk transport and kinetic phenomena. Further, they should form the basis for accurately assessing component and electrode failure modes and lay a path for advancements.

Supported by diagnostic studies, materials development on silicon-based materials, electrodes, and cells is being conducted to enhance interfacial stability, accommodate intermetallic volume changes, and improve overall performance and life. Key to this effort is the development and testing of coatings and additives designed to modify and stabilize the dynamic silicon-electrolyte interface. Further, functional polymer binders designed to accommodate volume changes, increase conductivity, and improve adherence are being developed and analyzed. Finally, the program is exploring active material development, including high-energy silicon and silicide materials, development of additional lithium inventory additives, and use of designer passivation materials.

Communication of programmatic progress to battery community is critical. This will generally be accomplished through publications, presentations, reports, and reviews. Further, the program is open to industrial participation and/or collaboration that does not limit program innovation or the free flow of information. Finally, this program is highly integrated with our sister program on SEI-Stabilization (SEISta). In general, SEISta is focused on the development and characterization of model systems, thin-film well-defined active area electrodes on which it is easier to extract fundamental information on lithium-silicon phase formation, lithium transport, and interfacial phenomena (e.g. SEI formation and growth).

Milestone FY2019 Q2

Demonstrate that controlling lithium inventory in a full cell can extend cycle life of a silicon-based electrode by at least 10%.

Within the DeepDive Silicon effort, we have been seeking to understand how cell balancing (n:p ratios) and the use of pre-lithiation reactions is tied to cell performance. For pre-lithiation studies, Wenquan Lu and Chris Johnson have evaluated the utility of adding a one-time source of active lithium to the cathode laminate. By adding Li_5FeO_4, which undergoes disproportionation to 2 Li_2O + $LiFeO_2$, the amount needed to offset first cycle losses can be can be controlled and built into the cathode electrode structure. Although discussed for this FY19Q3 update, for reasons associated with laminate fabrication and loss of energy density, this pathway has been discontinued but is discussed here for completeness of the options considered. Jason Zhang has evaluated utilizing a lithium anode for the formation cycles against a Si-based electrode and then rebuilding the cell with this formed Si-based anode and a conventional NMC cathode. A third avenue has been the focus of the CAMP team and Dan Abrahams group where the cathode to anode electrode active material amount was varied to control the n:p ratio and thus the amount of lithium available.

Summary: In Q3, we have addressed issues associated with cycling efficiency and loss of active lithium. The loss of lithium is a critical issue for silicon-based electrodes as it is closely associated with the commonly observed large first cycle irreversible capacity loss (typically > 20%) that robs the cell of available lithium and contributes to electrode voltage drifting (cathode becomes over oxidized). There are three approaches the DeepDive effort has evaluated in FY19, adding extra lithium to the cathode, sacrificial lithium at the anode, and using cell balancing to bring more lithium to the couple.

Extra cathode-based lithium: Within this area, work by Johnson and Lu initially focused on the role of adding a one-time source of active lithium to the cathode during the lamination process. This method has the advantage that, assuming the amount of first cycle irreversible capacity is roughly constant for an electrode, the amount of extra lithium can be tailored to match the deficit created after the first cycle. In their studies, the one-time source

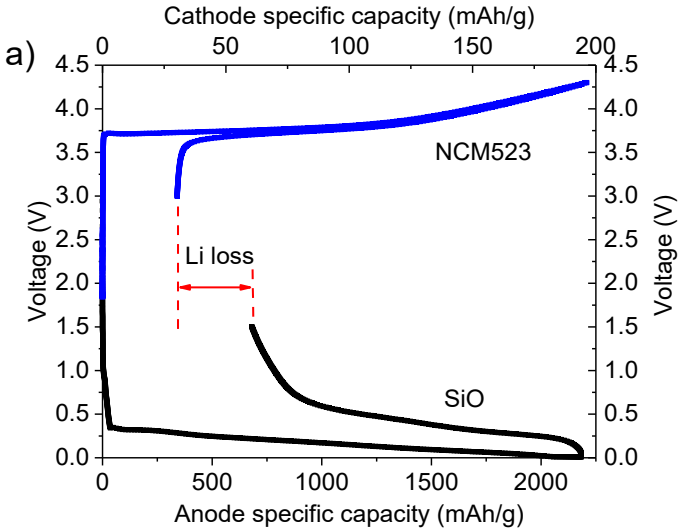

Figure 2 Full cell matching for SiO/NCM523

of extra lithium was the compound Li_5FeO_4 (LFO), as noted above, while the silicon used was a commercial "SiO" material (HydroQuebec) chosen for its consistency and high first cycle irreversible capacity.

Based on the first cycle voltage profiles, the amount of LFO needed to compensate the Li loss of SiO is calculated to be approximately 10% of the NCM523 weight. In **Figure**s 2 and 3, the two scenarios of full cell matching

considering an n:p ratio of 1 are considered. **Figure** 2a shows the scenario when a SiO anode is paired with an NCM523 cathode, and due to the difference in the first cycle coulombic efficiency and therefore the initial

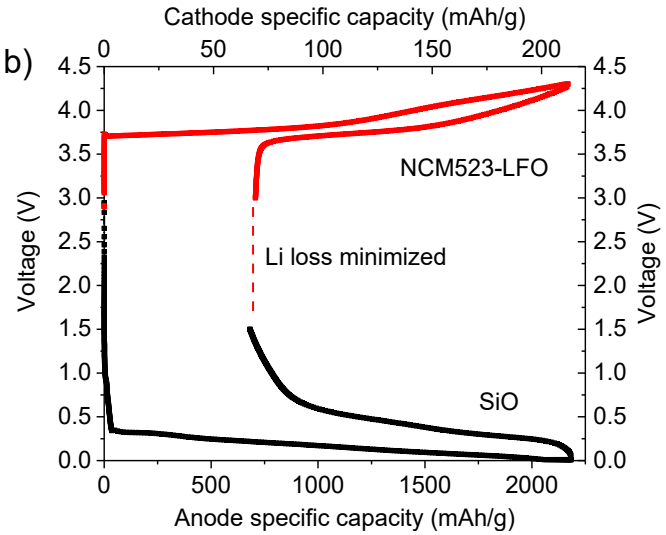

Figure 3 Full cell matching SiO/NCM523-LFO

capacity loss, a significant portion of lithium extracted from the NCM523 cathode is used towards parasitic reactions in the SiO anode, as noted in **Figure** 2. This loss of lithium to irreversible parasitic reactions leads to low Li utilization for the reversible cycling and lower capacity of the cell. In **Figure** 3, a cell was built to offset that first cycle irreversible capacity loss by LFO addition to the NMC523 laminate.

On cycling, the comparison between the two options is more easily seen (see **Figure** 4). By using non-cathode active lithium to offset the first cycle irreversible capacity losses seen for silicon, the amount of lithium lost to side reactions from the NMC523 cathode is minimalized. The specific capacity of SiO/NCM523-LFO full cells shown in **Figure** 3 is based on the weight of NCM523-LFO blend.

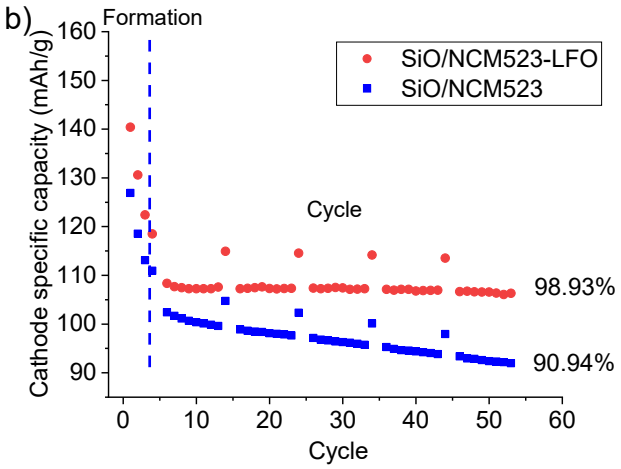

Figure 4 cycle performance comparison of NCM523/SiO and NCM523-LFO/SiO. The capacity of SiO/NCM523-LFO full cells are calculated based on the total weight of NCM523-LFO blend

This offset by LFO addition leads to a 22% more lithium utilization from NCM523, and an 11% improvement in the discharge capacity of the cell. Notably, the capacity fade seen in the initial three formation cycles for both SiO/NCM523 and SiO/NCM523-LFO, has been attributed to lithium trapping in the cycled "SiO". During the cycle test, SiO/NCM523 showed a capacity retention of 90.94% for 50 cycles, while the addition of LFO improved the capacity retention to 98.93% for 50 cycles. Furthermore, the reversible capacity was improved from 102.4 mAh/g for SiO/NCM523 to 119.7 mAh/g for SiO/NCM523-LFO at the start of the cycle test, or 16.9% improvement in lithium utilization from NCM523.

Prelithiation with a sacrificial anode: Although typically utilized as part of an analytical technique to assess electrode changes on long term cycling, using a sacrificial lithium source to pre-make the SEI on the Si anode can be used to minimize the effect of the first cycle irreversible capacity on the cell cycling lifetime. This technique has been used in the DeepDive silicon effort at PNNL (Zhang Group) and ANL (Abraham Group). The method involves building a cell with the silicon-based electrode and a sacrificial lithium metal anode. After formation cycling, the cell is disassembled and the cell is rebuilt with an NMC cathode (with a cycled silicon anode). The Zhang group has been investigating the use of alternative electrolytes based on fluoride-containing solvent systems. The required binder is a poly-imide (PI) based system that when combined with silicon has a high first cycle irreversible capacity. Experimentally the first cycle efficiency of their BTR1000 silicon anode utilized was ~ 80%, so to offset this loss the anode was pre-lithiated by cycling against Li metal for 3 cycles and the silicon electrode was isolated after charging to 1.5 V. The *pre-lithiated* anodes were paired with an NMC333 cathode to form the full-cells used. Using these anodes and their top formulation, NFE-2 (1.2M LIFSI in (TEP-FEC)-3BTFE + 1.2wt% FEC), a capacity retention of 98.2% over 200 cycles was recorded.

Cell Balancing: Cell balancing utilizes the deliverable capacity of the positive (p) and negative (n) electrode to optimize the amount of cycling lithium in a cell. This cell-based technique seeks to maximize the cathode and anode chemistry so that each electrode, after formation, delivers (or accepts) lithium within its most stable and desirable voltage range. Moving off this ratio over-oxidizes the cathode (average voltage moves up) or over-reduces the anode (i.e. lithium plating). If in the case of a silicon anode the first cycle irreversible capacity is high enough that various efforts to balance cells have been undertaken. Previously Vaughey, Dogan, Trask, and Key (FY19Q1) utilized the high capacity HE5050 cathode (> 210 mAh/g) to push cell balancing with their new

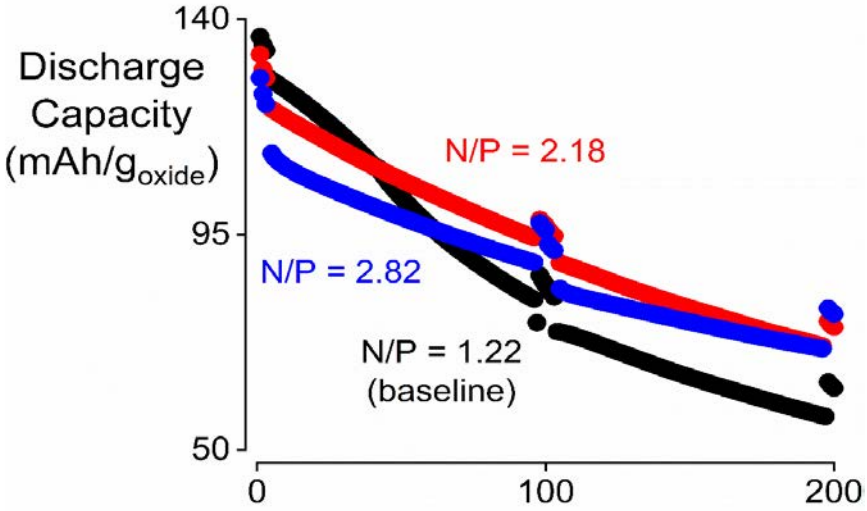

Figure 5. Discharge capacity vs. cycle number for NCM523/15Si cells, with various n:p capacity ratios: 1.22 (black plot, our baseline), 2.18 (red plot) and 2.82 (blue plot), tested at 30°C. The test protocol contained two repetitions of 100 cycles. In each of these 100 cycles, cycles 1-3 are at a ~C/20 rate, 4-97 are at a ~C/3 rate and 98-100 are at a C/20 rate.

Mg-Zintl additives as NMC532 (~160 mAh/g) was found to provide inadequate electrode capacity limiting the depth of silicon used. In this detailed study, Abraham et al., varied the n:p ratio (NMC532 cathode, 15%Si

anode) from the baseline value near 1 to 3 to evaluate the role of over-sizing the anode and change the amount of lithium available to the silicon/graphite in the composite anode creating a LiSi/Gr matrix. In **Figure** 5, the discharge capacity vs. cycle number plots for the various cells are shown: all capacities are listed as mAh/g-oxide, wherein the oxide refers to the weight of the NCM523 component in the positive electrode. The Coulombic efficiencies (CE) for cells with n:p ratios of 1.22, 2.18 and 2.82 were 76%, 70% and 67%. Since CE's did not decrease in proportion to the increasing the amount of anode relative to the cathode (n:p) ratio and the capacities after 200 cycles were 20-25% greater for cells with the higher n:p ratios, we believe that the SEI losses in thicker electrodes are offset by the greater capacity retention. As the anode is incompletely utilized in this study as the amount of anode is increased, lower volume expansion and material pulverization is observed which may be acting to restrict the surface area of the silicon leading to less SEI forming on the anode surface.

Overall, the goal of this FY19Q3 milestone to demonstrate the utility of pre-lithiation as a method to increase cycling efficiency has been evaluated using three different methods. Options including laminate modification, sacrificial anodes, or utilizing less of the available silicon (via n:p ratio control) have been evaluated. The goal of eliminating some of the detrimental effects of first cycle inefficiencies has been met but the offsetting associated costs tied to the options we evaluated make it a difficult, at this time, to dedicate the resources necessary to incorporate it into our baseline DeepDive cells.

Silicon - Containing Anodes with Extended Cycle Life and Calendar Life (PNNL)

Ji-Guang Zhang, Xiaolin Li

Background

Highly porous structured Si has been widely used to avoid pulverization of Si particles during cycling process. However, the large surface area of nano Si or micron sized porous Si may also leads to an enhanced rate of reaction between lithiated Si and electrolyte leading to continuous SEI growth and an increase of cell impedance. Another possible degradation mechanism is the cross talk between Si anode and cathode. An FEC additive, which is highly effective in forming a stable SEI layer on Si, may form a detrimental cathode electrolyte interface (CEI) on cathode surface which also leads to impedance increase. Therefore, minimize the surface area of Si and find a stable electrolyte additive are critical for long term stability of Si based Li-ion batteries.

In this project, we will enhance the cycle life and calendar life of Si based Li-ion batteries by designing a stable porous Si structure with a more stable SEI layer. A more stable electrolyte additive or solvent mixture will be developed to minimize the detrimental effect of FEC currently used in Si based Li-ion batteries. The degradation mechanism of Si anodes during shelf storage will be systematically investigated.

Results

In last quarter, localized high concentration electrolytes (LHCEs) of 1.8M LiFSI in (EC-EMC) - 2BTFE (BTFE is bis-trifluoroethylether) has been demonstrated to enable long-term cycling (82.1% retention over 200 cycles) and high voltage stability (up to 4.5V for NMC532‖ Li cells) using Si anodes prepared by CAMP facility. This demonstrates that LHCEs can enable the formation of a more stable SEI on the surface of silicon than those of baseline Gen2+FEC electrolyte. In this quarter, LHCEs were modified by addition of triethyl phosphate (TEP), a non-flammable solvent, and compared to LHCEs with carbonate solvents were further investigated for Si based anodes. Because TEP is not compatible with LiPAA binder used in the CAMP Si anodes, polyimide (PI)-type binders were used to prepare our Si anodes in combination with a commercially available nano-Si/graphite composite (BTR1000) from BTR New Energy Materials (Tianjin). The first cycle efficiency of the BTR1000 silicon anodes was ~ 80%. To enable the full cycle operation, the anode was pre-lithiated by cycling against Li metal for 3 cycles. The voltage window for the prelithiation was 0.02-1.5 V and the anodes were collected after they were de-lithiated to 1.5 V. The pre-lithiated anodes were paired with an NMC333 cathode to form the full-cells used in this study. The non-flammable electrolytes tested are listed in Table 1. The areal capacity of the full cells at 0.75 mA cm^{-2} is 1.5 mAh cm^{-2}. As shown in **Figure** 6a, BTFE diluent works better than TTE (TTE - 1,1,2,2-tetrafluoroethyl-2,2,3,3-tetrafluoropropylether) diluent, a common additive for Li-S cells added for lithium protection. Table 1 lists the abbreviations for the various electrolyte muixtures. NFE-2 with only 1.2 wt% FEC demonstrated the best cycling stability with the capacity retention of 98.2% over 200 cycles (**Figure** 6b). When FEC content increases to 5 wt%, the cells exhibited quick capacity drop. In another effort, carbonate solvents (EC-EMC, DMC) based LHCEs were investiged using BTR1000 electrodes. The composition of the electrolytes is shown in Table 2. As shown in **Figure** 7, the new carbonate-based LHCEs for BTR1000‖NMC532 full-cells demonstrate good cycling stability up to 200 cycles. DMC based LHCEs also exhibited higher capacity compared to that based on EC-EMC based LHCEs. The above results further confirm that LHCEs can effectively improve the cycling stability of silicon anodes. Molecular dynamic simulation and surface characterization of Si anodes are undergoing to understand the mechanism for improved cycling stability.

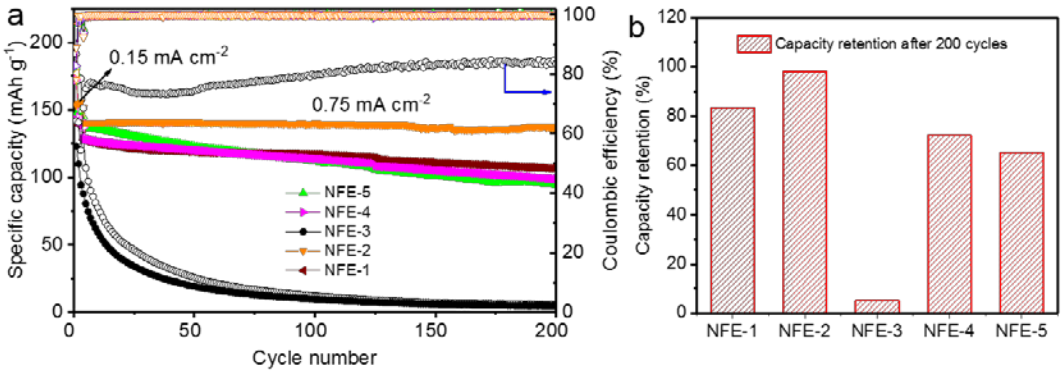

Figure 6. (a) Long-term cycling performance of BTR1000|| NMC333 full-cells in non-flammable LHCEs. (b) Capacity retention of full cells in non-flammable LHCEs.

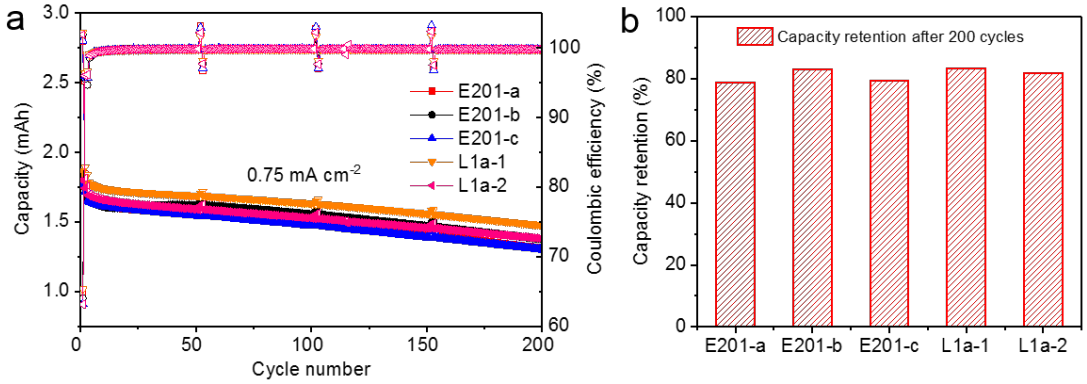

Figure 7. (a) Long-term cycling performance of BTR1000|| NMC532 full-cells in carbonate-based LHCEs. (b) Capacity retention of full cells in carbonate-based LHCEs.

Table 1. Composition of non-flammable LHCEs investigated in this work

Nonflammable LHCEs	
NFE-1	1.2M LIFSI in TEP-3BTFE
NFE-2	1.2M LIFSI in (TEP-FEC)-3BTFE (including1.2wt% FEC)
NFE-3	1.2M LIFSI in TEP-3BTFE+ 5wt%FEC
NFE-4	1.2M LIFSI in TEP-2TTE
NFE-5	1.2 M LIFSI in TEP-2TTE+ 5wt%FEC+1wt% VC

Table 2. Composition of the carbonate-based LHCEs investigated in this work

Carbonate based LHCEs	
E201	LiFSI in EC-EMC (3:7 by wt%)
E201-a	E-201+1.72TTE+5wt%FEC+1wt% VC
E201-b	E-201+1.29 S1+5wt% FEC+ 1wt% VC
E201-c	E-201+2.2 S1+5wt5 FEC+ 1wt%VC
L1a	LiFSI in DMC
L1a-1	L1a+1.29 S1+5wt% FEC+ 1wt% VC
L1a-2	L1a+2.2 S1+5wt FEC+ 1wt%VC

Conclusions

For the commercial BTR1000 silicon-based anodes with a poly-imide (PI) binder, both TEP- and carbonate-based LHCEs enables good cycling stability after a prelithiation process. For TEP-based LHCEs, BTFE diluent works better than TTE. The addition of optimized amount of FEC additive in LHCEs can further enhance the electrochemical performance of Si based anode. BTR1000|| NMC333 full-cells with NFE-2 electrolyte which contain only 1.2 wt% FEC demonstrate the best cycling stability with the capacity retention up to 98.2% over 200 cycles.

References

- Haiping Jia, Lianfeng Zou, Peiyuan Gao, Cao Xia, Wengao Zhao, Yang He, Mark H. Engelhard, Sarah D. Burton, Hui Wang, Xiaodi Ren, Qiuyan Li, Ran Yi, Xin Zhang, Chongmin Wang, Zhijie Xu, Xiaolin Li, Jiguang Zhang, Wu Xu "High performance silicon anodes enabled by nonflammable localized high concentration electrolytes,", Advanced Energy Materials (2019) https://doi.org/10.1002/aenm.201900784

Processing Conditions and their Effect on Silicon-based Anodes (ORNL)

Katie Burdette (ORNL), Alex Rogers (ORNL), Beth Armstrong (ORNL), and Gabriel Veith (ORNL)

Background

The surface of silicon is highly dependent on the synthesis method and processing conditions. Two different silicon samples - (1) Paraclete Lot #F17-021-LS and (2) Paraclete Lot #G18-031-MM—made with different processing conditions were examined to elucidate the role that silicon surface plays in electrode processing and electrochemical testing. Each silicon was characterized using zeta potential, rheology, and electrochemical cycling. Understanding the silicon surface will allow for more uniform electrodes to be fabricated, which will lead to an enhancement in electrochemical performance.

Results

Zeta potential of two different silicon powders (Paraclete Lot #F17-021-LS and Paraclete Lot #G18-031-MM) to determine the effect of powder changes on stability and role of silicon surface in electrode architecture. The zeta potential of Paraclete Lot #F17-021-LS and Paraclete Lot #G18-031-MM as a function of pH is given in **Figure** 8. The isoelectric point, i.e. the point at which zeta potential is zero and there are no repulsive forces present in the dispersion, is ca. pH 2 for Paraclete Lot #F17-021-LS and is ca. pH 3.5 for Paraclete Lot #G18-031-MM. As discussed by Parks et. al. the isoelectric point indicates that the SiO_2 on the surface of Paraclete Lot #F17-021-LS, is more crystalline, while the SiO_2 of Paraclete Lot #G18-031-MM is more "gel-like" or

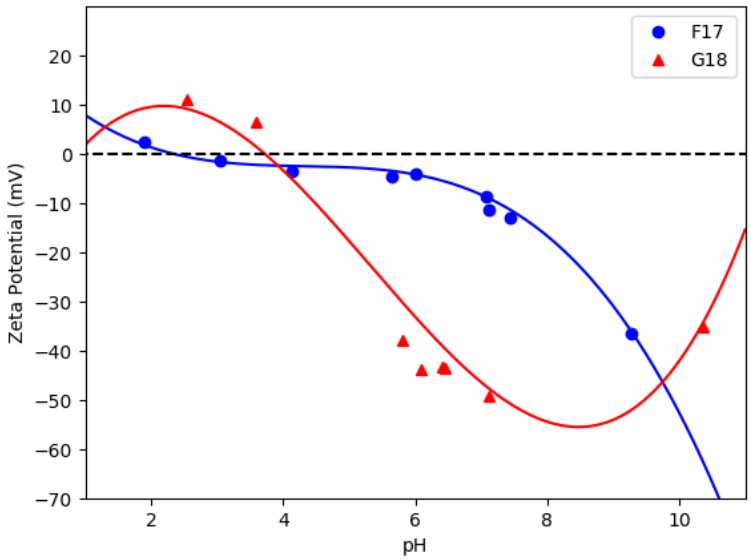

Figure 8: Zeta potential as a function of pH for Paraclete Lot #F17-021-LS (blue) and Paraclete Lot #G18-MM-031 (red). The black line represents the isoelectric point. Paraclete Lot #F17-021-LS is not electrostatically stable while Paraclete Lot #G18-MM-031 is electrostatically stable over the working pH range of electrode slurries (pH 5-8).

amorphous.[1] Paraclete Lot #F17-021-LS is not electrostatically stable until a pH of 9 is reached while Paraclete Lot #G18-031-MM reaches electrostatic stability at pH 5. The surface of Paraclete Lot #G18-031-MM facilitates a more stable dispersion as its average zeta potential over the working pH range (pH 5-8) over of the slurries is ca. -45 mV while that of Paraclete Lot #F17-021-LS is ca. -10 mV. In the working pH range of the electrode slurries, Paraclete Lot #G18-031-MM will remain more dispersed in the slurry while Paraclete Lot #F17-021-LS will agglomerate. Agglomeration in the slurries leads to silicon peaks and valleys and a non-uniform electrode that will lithiate certain areas of the electrode selectively. To further investigate flow behavior of the

nanopowders, rheology was performed on electrode slurries containing either Paraclete Lot #F17-021-LS or Paraclete Lot #G18-031-MM silicon.

Figure 9 presents viscosity as a function of shear rate for Paraclete Lot #F17-021-LS and Paraclete Lot #G18-031-MM electrode slurries. Each slurry contained water, 37 wt% silicon, 2 wt% carbon black, 10 wt% PAA

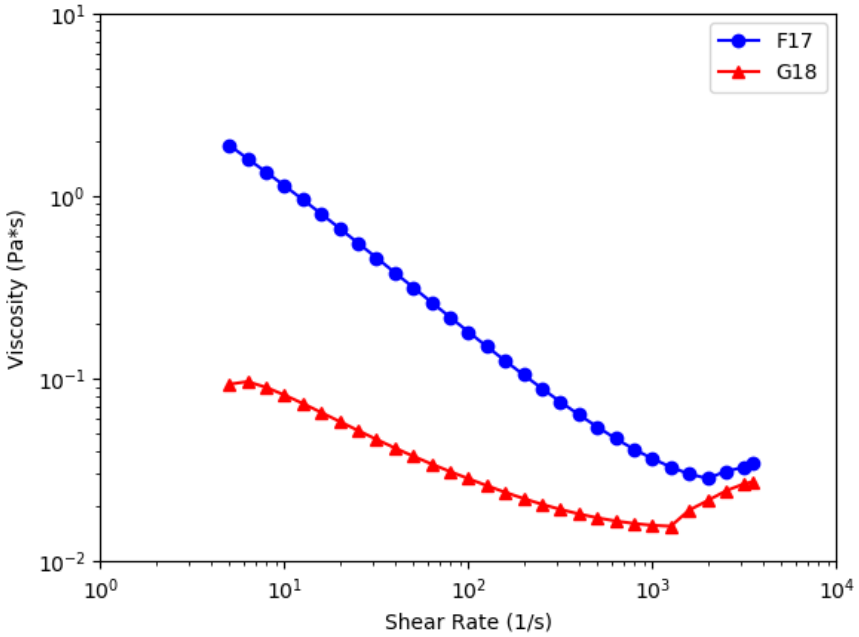

Figure 9. Viscosity as a function of shear rate of electrode slurries made from 250k poly(acrylic acid), 1.8k poly(acrylic acid), either Paraclete Lot #F17-021-LS (blue) or Paraclete Lot #G18-031-MM (red), carbon black, and water.

binder (250k g/mol molecular weight), and 1 wt% PAA dispersant (1.8k g/mol molecular weight). At low shear rates (5 Hz to 50 Hz), the viscosity of Paraclete Lot #F17-021-LS is over one order of magnitude more viscous than Paraclete Lot #G18-MM-031. The initial viscosity of Paraclete Lot #F17-021-LS is approximately 2 Pa s, while the viscosity of Paraclete Lot #G18-031-MM ca. 0.01 Pa s. The surface of Paraclete Lot #F17-021-LS is likely made of more crystalline SiO_x which can form intra- and inter-molecular hydrogen bonds, leading to higher viscosities. The surface of Paraclete Lot #G18-031-MM is likely covered with less crystalline SiO_x and more nonpolar moieties, leading to an overall lower viscosity due to the dilution of hydrogen bonds.[2] While the overall viscosity of Paraclete Lot #G18-031-MM is lower than that of Paraclete Lot# F17-021-LS, the onset of shear thickening begins at ca. 1000 Hz and ca. 2000 Hz for Paraclete Lot #G18-031-MM and Lot #F17-021-LS, respectively. The shear thickening response is also more pronounced in Paraclete Lot #G18-031-MM than in Lot #F17-021-LS. While shear thickening in colloidal suspensions is still debated, the magnitude of this shear thickening is likely due to hydrocluster formation. Under high shear rates, the particles flocculate together and there is increased drag between the particles that they must overcome to move.[3] The difference in shear thickening could be due to larger repulsion forces. To prevent agglomeration, care must be taken to cast the electrodes below this threshold. ORNL is working with the CAMP facility to determine the rate at which their electrodes are cast. Chemical characterization of the surface of these materials is ongoing.

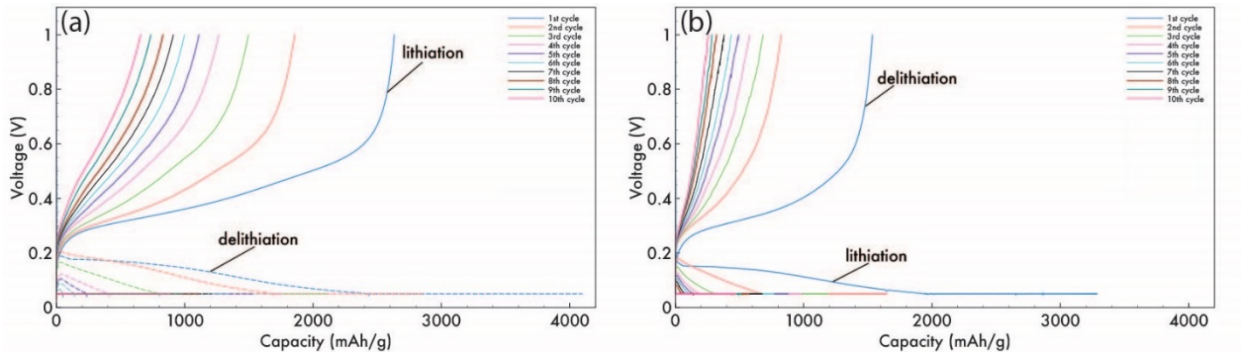

Figure 10: Voltage versus mass normalized capacity during lithiation and delithiation of the first 10 cycles of electrodes made with (a) Paraclete Lot #G18-031-MM or (b) #F17-021-LS. Paraclete Lot #G18-031-MM has superior electrochemical performance when compared to Lot #F17-021-LS.

Electrochemical testing of the aforementioned silicon electrode slurries was performed where coin half cells (against lithium) were cycled at a C/3 rate., see **Figure** 10. Electrodes fabricated from Paraclete Lot #G18-031-MM had greater first cycle capacity (4096 mAh/g versus 3286 mAh/g), greater capacity retention (second cycle capacity fade of 31% versus 50%), and Coulombic efficiency (64% versus 47%) than electrodes made from Paraclete Lot #F17-021-LS. The differences seen in zeta potential and rheology in the Paraclete surfaces are reflected in the electrochemical performance. Chemical characterization (XPS, IR) of the electrodes to determine the cause is also ongoing.

Conclusion

The surface of silicon was elucidated and used to predict electrochemical performance. These results are being fed back to Argonne National Lab and comparison on processing conditions between the ORNL silicon electrodes and ANL silicon electrodes is ongoing.

References

1. Parks, G., The Isoelectric Points of Solid Oxides, Solid Hydroxides, and Aqueous Hydroxo Complex Systems. *Chemical Reviews* **1965,** *65* (2), 177-198.
2. Christensen, G.; Younes, H.; Hong, H. P.; Smith, P., Effects of solvent hydrogen bonding, viscosity, and polarity on the dispersion and alignment of nanofluids containing Fe2O3 nanoparticles. *Journal of Applied Physics* **2015,** *118* (21).
3. Brown, E.; Jaeger, H. M., Shear thickening in concentrated suspensions: phenomenology, mechanisms and relations to jamming. *Reports on Progress in Physics* **2014,** *77* (4).

Binders and Surfaces for Composite Silicon-Based Electrodes (ANL)

Zhangxing Shi, Lu Zhang (Argonne National Laboratory)

Background

As a Li-storage material, silicon (Si) has relatively low cost and higher theoretical capacity (4200 mAh/g) compared to the conventional Li-intercalation anode material graphite (372 mAh/g). However, commercial use of Si-based anodes has been hindered by its large volumetric expansion (ca. 320%) during lithiation/delithiation processes, which leads to unstable solid-electrolyte interphase (SEI), rapid loss of cohesion in the electrode matrix, and particle pulverization. To mitigate these problems, compatible polymer binders including alginate, sodium carboxymethyl cellulose, poly(vinyl alcohol), polyimide, and poly(acrylic acid) (PAA) have been utilized to provide strong adhesion between the active materials (graphite and/or Si) and conductive carbon particles and accommodate the severe volume changes. Among them, PAA stands out due to its promising performance and was selected as the standard binder material for the Silicon Deep Dive program. Although PAA outperforms most reported binders, the factors affecting its performance are not fully understood and the reported performance is still far from meeting the requirement of practical use. Therefore, it is important to gain in-depth understanding of the performance of PAA based binders and evolving these binders towards desired cell performance for silicon lithium-ion batteries.

Pre-lithiation of PAA binders is a common strategy for fabricating silicon negative electrodes, which could benefit the large-scale lamination process and enable the fabrication of mechanically robust electrodes. The viscosity of PAA solution increases significantly with pre-lithiation and that potentially leads to improved slurry stability. However, the lithiation process utilizes lithium hydroxide (LiOH), which dramatically raises the pH of the resulting PAA solution. The lithiation process also changes the chemical properties of PAA binder by replacing carboxylic acid groups with carboxylate groups. These variations may adversely affect Si chemical stability, binding strength of PAA, and cell performance. Therefore, improving the viscosity of the binder solution to enhance the slurry stability but with no or minimum pH increase and chemical modifications of PAA binder would be highly desirable. In addition, the role of processing solvents for electrode lamination is very important but the understanding is very limited. For instance, in our preliminary studies, electrodes made with two common processing solvents (i.e., N-Methyl-2-pyrrolidone (NMP) and water) showed significant difference in cell performance. Therefore, we propose three approaches to investigate and develop high performance binders for silicon lithium-ion batteries as well as build understanding of their behaviors. **Firstly**, weak bases such as ammonia (NH_3) and triethylamine (Et_3N) were used as temporary additives to tune the viscosity of PAA solutions. **Secondly**, the solvation behavior of PAA in various solvents have been investigated by small-angle X-ray scattering (SAXS). The fabricated electrodes using these binder/processing solvent systems were evaluated in Li half cells. **Thirdly**, PAA analogues (e.g., poly(ethylene-alt-maleic acid), poly(malic acid), etc.) were pursued as new binder materials with modified properties.

Results

When dissolved in water, lithiated PAA solutions have significantly improved rheological properties than straight PAA solutions at the same concentration (i.e., higher viscosity at low shear rate and better shear thinning at high shear rate). Our previous studies indicated that high viscosity of binder solution is beneficial to the stability of electrode slurry. For instance, lithiated PAA solution has much higher viscosity than straight PAA solution, and it requires more water added to the slurry to achieve the desired state for lamination. The water added to PAA-85%Li (85% acid groups of PAA are lithiated) slurry is three times of that of straight PAA slurry when using 1.2 g of active materials, therefore the PAA-85%Li slurry could be more stable due to better dispersion of electrode materials and less impact of water evaporation. However, electrodes with lithiated PAA binders suffer more capacity loss in both half cells and full cells because of the increased pH value of the binder

solution and weaker binding strength. To improve the viscosity of the PAA binder solution while minimizing the unfavorable effects, weak bases (e.g., NH_3 and Et_3N) were added as temporary additives to neutralize PAA instead of LiOH. These bases are supposed to tune the viscosity the similar way as LiOH does but with much reduced increase of pH. Additionally, these weak bases could be removed from the electrode by thermal decomposition during the drying process at high temperature (> 80 °C). Thus, the binding strength of PAA binder

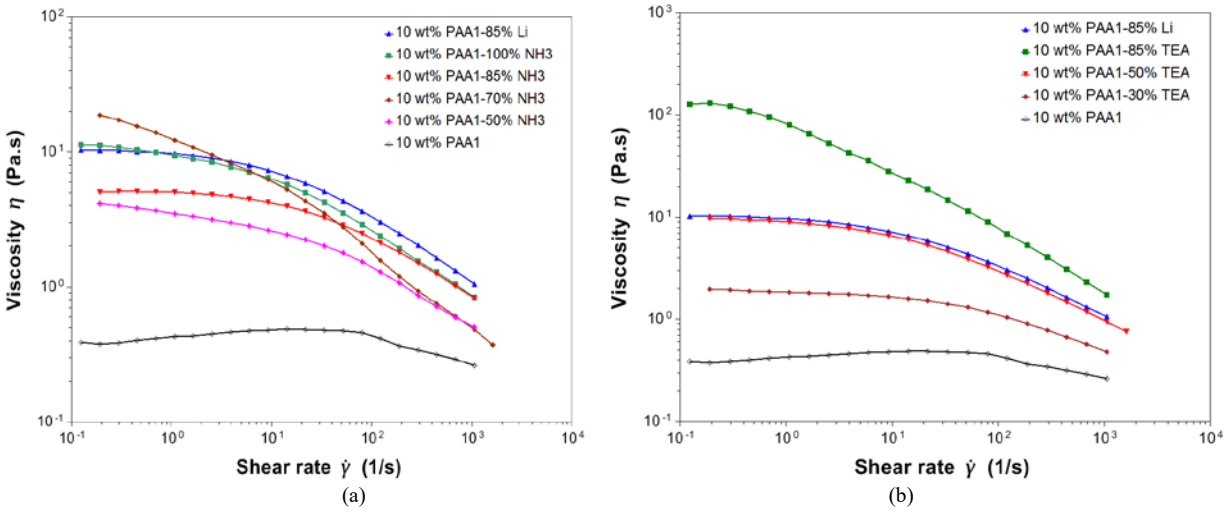

Figure 11. Plots of apparent viscosity vs. shear rate for 10 wt% aqueous solutions of (a) PAA mixed with $NH_3 \cdot H_2O$ and (b) PAA mixed with Et_3N. Straight PAA and PAA-85%Li were chosen as two baselines for comparison.

could be restored since the ammonium carboxylate groups will convert to carboxylic acid groups after thermal decomposition. As shown in **Figure 11a**, the rheology data of PAA solutions neutralized by NH_3 (i.e., PAA-NH_3) is comparable with the current standard PAA-Li binder used by CAMP (i.e., PAA-85%Li with pH of 6). Importantly, PAA-NH_3 solutions have lower pH values than PAA-85%Li due to the hydrolysis of NH_4^+ cations

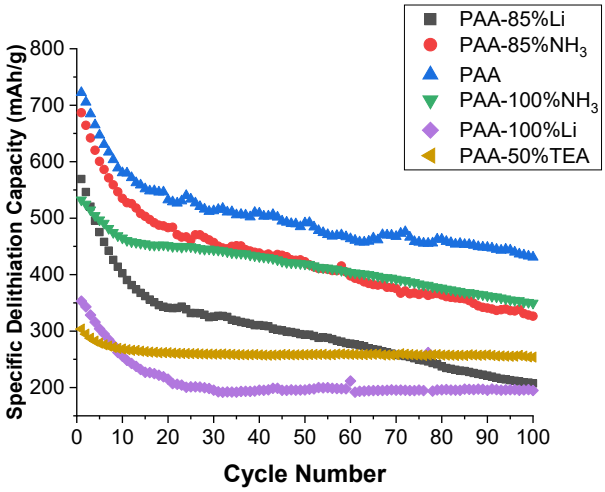

Figure 12. Specific delithiation capacity profiles of half cells using electrodes containing 73 wt% graphite, 15 wt% Si, 10 wt% modified PAA binders, and 2 wt% C45 over 100 cycles at C/3 rate.

(e.g., pH of PAA-85%NH_3 is 5). PAA solutions modified by Et_3N (i.e., PAA-TEA) showed even more promising viscosity improvements because of the bulky Et_3NH^+ cations. For example, PAA-TEA solution with only 50% of Et_3N achieved similar viscosity and shear thinning as PAA-85%Li solution. Since less base was needed to achieve the desired viscosity, the pH of PAA-50%TEA solution is even lower (pH = 4.5).

The capacity profiles of graphite-Si composite (15 wt% Si) electrodes made with these modified PAA binders were summarized in **Figure 12**. The cells were subjected to three formation cycles between 0.01 V and 1.50 V at C/20 rate, followed by 100 cycles at C/3 rate. After formation cycles, PAA-50%TEA cells have much lower initial capacity (ca. 303 mAh/g) than straight PAA cells (ca. 722 mAh/g) and PAA-85%Li cells (ca. 569 mAh/g). The majority of the capacity provided by Si was lost during formation cycles, which implied that PAA-TEA binders may have very poor binding performance. This is possibly due to the overly large triethylammonium cations that could interfere with the binding interactions. As shown in **Figure 12**, PAA-85%NH_3 cells have higher initial capacity (ca. 686 mAh/g) and capacity retention than those of PAA-85%Li cells. Notably, PAA-100%NH_3 cells have slightly lower capacity than PAA-85%NH_3 cells during the first 50 cycles, then the performance of the two systems are very similar. On the other hand, PAA-100%Li performed the worst among the modified binders because of severe side reactions caused by high pH of binder solution (ca. 13) and weaker binding strength provided by lithium carboxylates. Overall, electrodes made with PAA-NH_3 binders showed significant improvements in cell performance compared to the current standard PAA-85%Li binder. Although the performance of PAA-NH_3 binders are not as good as straight PAA, the improved rheological properties of PAA-NH_3 binders could make them more suitable for practical applications. Since the PAA functional groups were supposedly restored after thermal decomposition of PAA-NH_3, the binding strength should be similar between PAA and PAA-NH_3. Therefore, the differences in cell performance of these binders are likely due to the distribution of binders in the electrode, which is related to the solvation behavior of binder molecules.
To investigate the solvation behavior of modified PAA binders, a series of 10 wt% binder solutions were

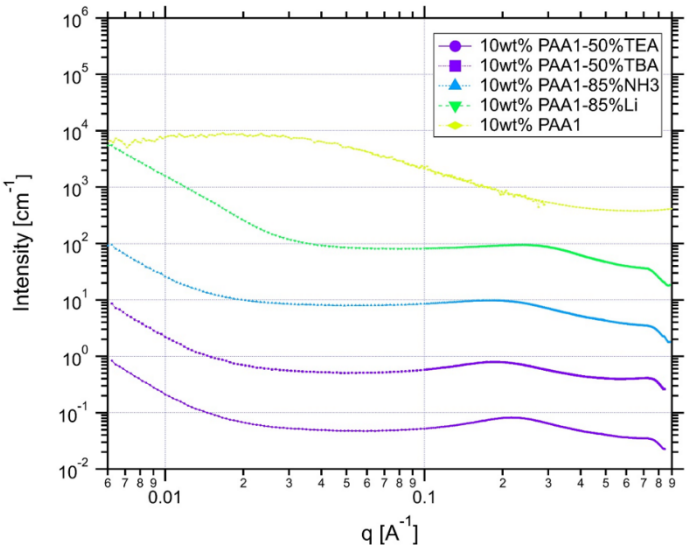

Sample	Rg (A)
10 wt% PAA1	31.63
10 wt% PAA1-85%Li	5.14
10 wt% PAA1-85%NH_3	5.36
10 wt% PAA1-50%TBA	6.41
10 wt% PAA1-50%TEA	5.03

(b)

Figure 13. (a) Small angle X-Ray scattering (SAXS) profiles for modified PAA solutions; (b) Sample information and Rg of the modified PAA solutions.

prepared for Small-angle X-ray scattering (SAXS) analysis in collaboration with Tao Li (Argonne National Laboratory) (**Figure 13a**). The radius of gyration (Rg) was calculated by applying unified fit to the broad peak composed of a Guinier part and a power law tail in each profile. As shown in **Figure 13b**, the results showed that Rg values dropped significantly by adding bases to PAA solution. For a given volume, smaller Rg indicates that the shape of the particle is more like sphere (i.e., smaller surface area for a given volume). Therefore, we suspect that large Rg values are beneficial to cell performance because the polymers are more stretched out and could interact with more active electrode materials. This could be one of the reasons why the performance of PAA-

NH_3 binders (Rg = 5.36) is not as good as straight PAA (Rg = 31.63) binder even though they are supposed to have the same chemical structure after drying process.

Sample	Rg (A)
10 wt% PAA1 in H_2O	31.63
10 wt% PAA1 in NMP	14.87
10 wt% PAA1 in Dioxane	15.98
10 wt% PAA1 in EtOH	15.95
10 wt% PAA1 in DMF	13.01
10 wt% PAA1 in Dioxane/H_2O	21.76

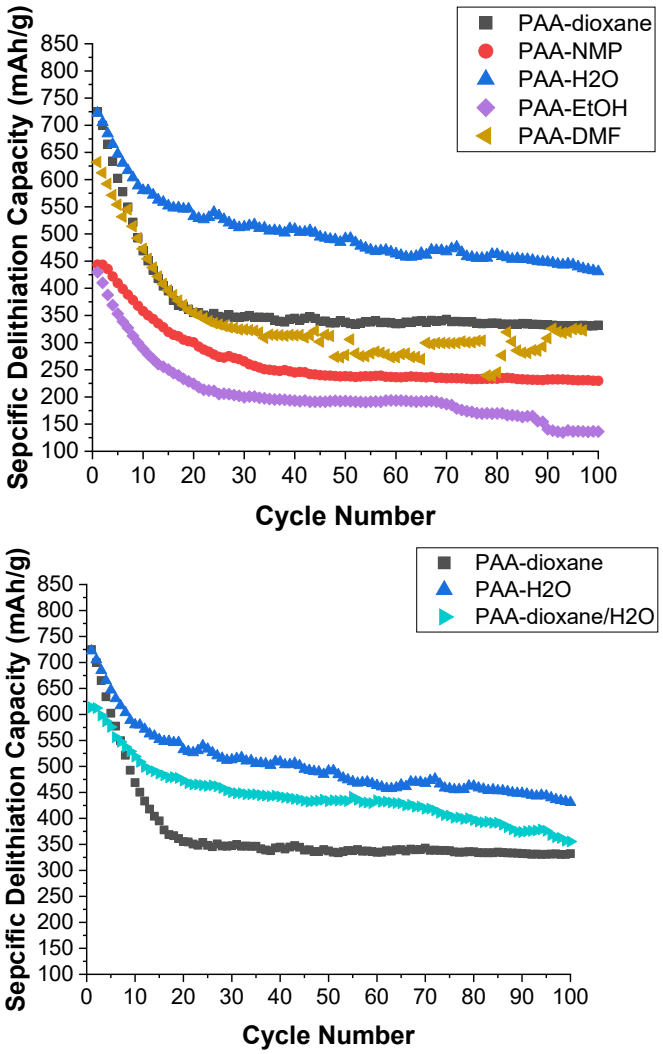

Figure 14. (a) Sample information and Rg of PAA solutions; (b) Specific delithiation capacity profiles of half cells using electrodes containing 73 wt% graphite, 15 wt% Si, 10 wt% PAA binders in organic processing solvent, and 2 wt% C45 over 100 cycles at C/3 rate; (c) Specific delithiation capacity profiles of half cells using electrodes containing 73 wt% graphite, 15 wt% Si, 10 wt% PAA binders in mixed processing solvent, and 2 wt% C45 over 100 cycles at C/3 rate.

It has been observed that the choice of solvent plays a big role in affecting the rheological properties of slurries and the cell performance, therefore it is extremely important to build a better understanding of the choice of processing solvents and hopefully to improve the current system. Several common organic solvents or organic

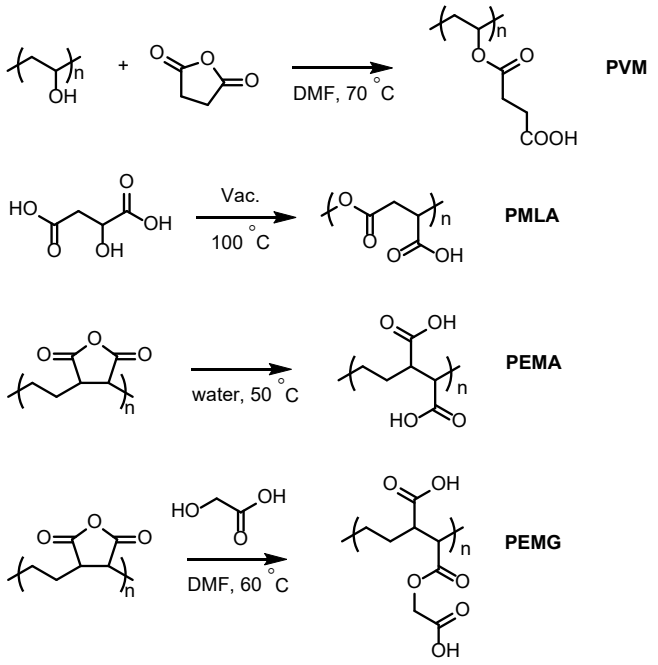

Figure 15. Synthetic scheme of PAA analogues as new binder materials.

solvent / water mixtures were firstly chosen as the processing solvent for lamination based on certain properties (e.g., solubility of PAA, clustering of PAA, and dielectric constant of the solvent). The prepared binder solutions showed visually improvements of viscosity except PAA-Ethanol solution. However, as shown in **Figure 14a**, the SAXS analysis indicated that the Rg values of PAA in these binder solutions are smaller than that of water solution, implying inferior cycling performance. The cycling characterization of Si/graphite composite electrodes fabricated using these processing solvents were conducted using our standard procedure: three formation cycles between 0.01 V and 1.50 V at C/20 rate, followed by 100 cycles at C/3 rate. As shown in **Figure 14b**, electrodes fabricated using 1,4-dioxane (PAA-dioxane) and *N,N*-dimethylformamide (PAA-DMF) have similar initial capacity compared to electrodes fabricated using water (PAA-H_2O) but suffer more severe capacity loss during the first 20 cycles. Electrodes fabricated using *N*-methyl-2-pyrrolidone (PAA-NMP) and ethanol (PAA-EtOH) showed significantly lower initial capacity than that of PAA-H_2O. It seems that water is still the best option among the tested solvents. Therefore, more combinations with water are pursued. For example, electrodes fabricated using mixture of equal weight of 1,4-dioxane and water (PAA-dioxane/H_2O) showed improved performance than PAA-dioxane, but not as good as PAA-H_2O. The Rg of PAA in 1,4-dioxane/water mixture also falls in between that of pure water and 1,4-dioxane, which is consistent with our hypothesis of the relationship of Rg and cell performance. At this point, the factors that make water such a superior processing solvent is still unclear. The outstanding performance of water might be a combined result of solubility, hydrolysis, pH, dielectric constant, and evaporation rate.

Finally, several PAA analogues were designed and synthesized as new binder materials including poly(monovinyl maleate) (PVM), poly(malic acid) (PMLA), poly(ethylene-alt-maleic acid) (PEMA), and

poly(ethylene-alt-maleic acid monoglycolate) (PEMG) (**Figure 15**). These new polymers have carboxylic acid group(s) in each repeat unit similar to PAA, but the solubility and T_g of these polymers are supposed to be different. The characterization and evaluation of these new polymers as binders for Si electrode is ongoing.

Conclusions

The balance between slurry stability and performance has been investigated by tuning the viscosity of PAA solution with weak bases such as NH_3 and Et_3N. Among these modified PAA binders, PAA-NH_3 showed promising viscosity improvement and cell performance for graphite-Si composite electrodes in half cell tests. The solvation behavior of PAA binders in organic solvents was explored using SAXS analysis and the results agree with our hypothesis that higher Rg values may favor better cycling performance. Si-graphite composite electrodes made with various PAA/processing solvent(s) combinations were evaluated in half cells. Electrodes fabricated using water outperformed electrodes fabricated using common organic solvents. Several new PAA analogues were designed and synthesized as new binder materials with modified properties. These new polymers will be evaluated as binders in the near future.

References

1. Wu H.; Cui, Y. *Nano Today* **2012**, *7 (5)*, 414-429.
2. Hu B.; Shkrob I. A.; Zhang S.; Zhang L.; Zhang J.; Li Y.; Liao C.; Zhang Z.; Lu W.; Zhang L. *J. Power Sources* **2019**, *416*, 125-131.
3. Erogbogbo F.; Lin T.; Tucciarone P. M.; LaJoie K. M.; Lai L.; Patki G. D.; Prasad P. N.; Swihart M. T. *Nano Lett*. **2013**, *13(2)*, 451-456.

Publications

- Bin Hu, Sisi Jiang, Ilya A. Shkrob, Jingjing Zhang, Stephen E. Trask, Bryant J. Polzin, Andrew Jansen, Wei Chen, Chen Liao, Zhengcheng Zhang, Lu Zhang "Understanding of pre-lithiation of poly(acrylic acid) binder: Striking the balances between the cycling performance and slurry stability for silicon-graphite composite electrodes in Li-ion batteries" Journal of Power Sources 416 (**2019**) 125–131.

Electrolytes and Additives

Gao Liu (LBNL)

Background

As a Li-storage material, silicon (Si) has relatively low cost and higher theoretical capacity (4200 mAh/g) compared to the conventional Li-intercalation anode material graphite (372 mAh/g). However, commercial use of Si-based anodes has This quarter we developed a polarity gradient solvent wash technique to better characterize the surface and near surface of a Cu planner electrode after exposed to electrolyte and subjected to 0.05 V (vs. Li/Li+) polarization. The electrolyte is either Gen2 without additives, or Gen2 electrolytes with 5% of the hydrophobic and hydrophilic electrolyte additives, developed earlier. The goals are to be able to expose the selective electrode surface for spectroscopy study, and extracted the selective side reaction products from the electrolyte and the surface of the electrode for chromatography and mass-spectrometry analysis.

Results

As a Li-storage material, silicon (Si) has relatively low cost and higher theoretical capacity (4200 mAh/g) compared The polarity gradient wash solvents are a series of gradient combination of ethylacetate (EA) and hexane (Hex) as shown in **Figure** 16. The polarity index of Hex is 0.1, the EA, 4.4. As a reference, the propylene carbonate solvent is 6.1. The polarity of the binary solvents of EA and Hex is proportional to the volume fractions of the two components. The lower polarity solvents combination can significantly slow down the dissolution of the polar byproducts, effectively separating the byproducts based on their polarity on the surface of the electrode and in the washed solutions.

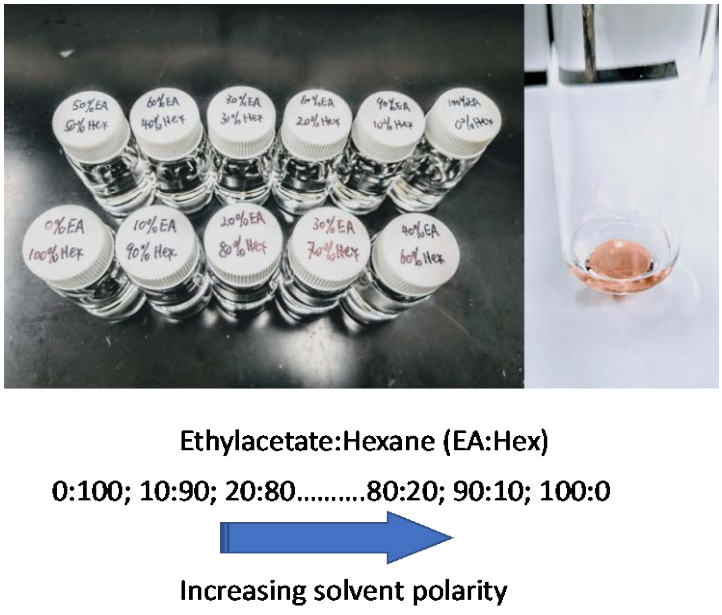

Figure 16. Gradient polarity solvent system setup (left) and electrode wash demo (right).

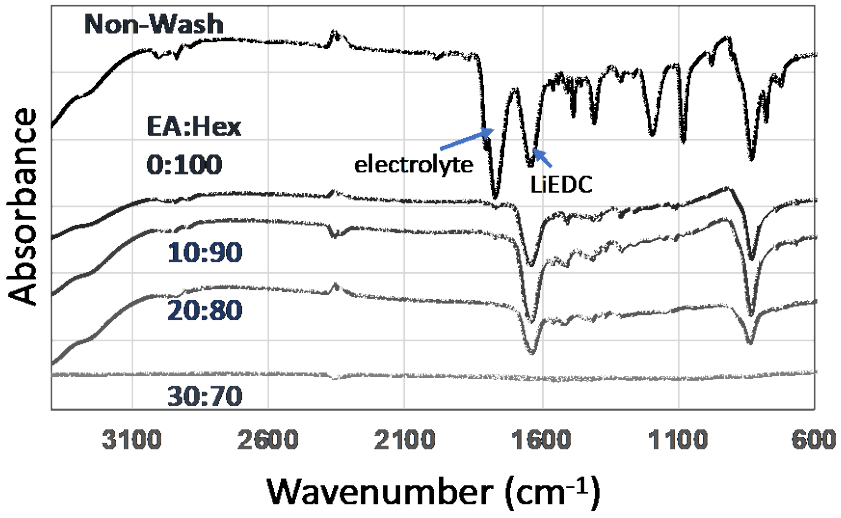

Figure 17. FTIR spectra of the Cu electrode surface subjected to gradient polarity solvent wash.

Conclusions

As a Li-storage material, silicon (Si) has relatively low cost and higher theoretical capacity (4200 mAh/g) compared. e demonstrated this technique on Cu electrode using a Gen2 electrolyte without additives. FTIR is used to observe the species on the surface of Cu electrode after 0.05V (vs. Li/Li+) polarization (**Figure** 17). The unwashed electrode shows strong electrolyte signals and LiEDC byproduct signals. At 20:80 ratio of EA/Hex of solvent wash, the electrolyte solvents are entirely removed from the surface, but the LiEDC still has very strong present on the surface of the Cu electrode. At 30:70 combination, both the electrolytes and LiEDC signals are entirely removed from the surface of the Cu. These results prove that the removal of the surface species is strongly correlate with the polarity of the wash solvent used. The method is used in the next quarters to study the decomposition of electrolyte additives on the electrodes.

Composite Silicon-Tin Anodes for Lithium-Ion Batteries (LBNL)

Wei Tong (LBNL)

Background

Thin films free of binder/conductive carbon additive offer the opportunity to enable the effective characterization of solid-electrolyte interphase (SEI) formation and evolution upon electrochemical cycling. In the last quarter, we successfully synthesized Si-Sn composite thin films of varied compositions by co-sputtering two separate Si and Sn targets using a multi-target sputtering instrument. In this quarter, we continued on characterizing the co-sputtered thin films by scanning electron microscopy (SEM), energy-dispersive X-ray spectroscopy (EDS), and electrochemical method to determine the optimal composition with superior cycling performance. The ultimate goal is to identify the promising Si-based thin film compositions and provide guidance for the synthesis of Si-based thin splats by splat quenching method.

Results

Si-Sn composite thin films were directly deposited onto the 12-μm-thick Cu foil by pulsed direct current (DC) magnetron co-sputtering using a 3-inch p-type Si target (99.999% purity) and 3-inch Sn target (99.998-99.999% purity). The film composition was controlled by adjusting the depositing power. All the as-deposited films were subsequently stored under vacuum to prevent air exposure. 2032-type coin cells were assembled using the as-produced films (1.6 cm^2) directly as the working electrode, Li metal foil as the counter electrode, and 1.2 M $LiPF_6$ in ethylene carbonate (EC)-ethyl methyl carbonate (EMC) (3:7 by weight) as the electrolyte (Gen2). The cells were galvanostatically cycled between 1.5 and 0.01 V at C/20 based on the experimental capacity.

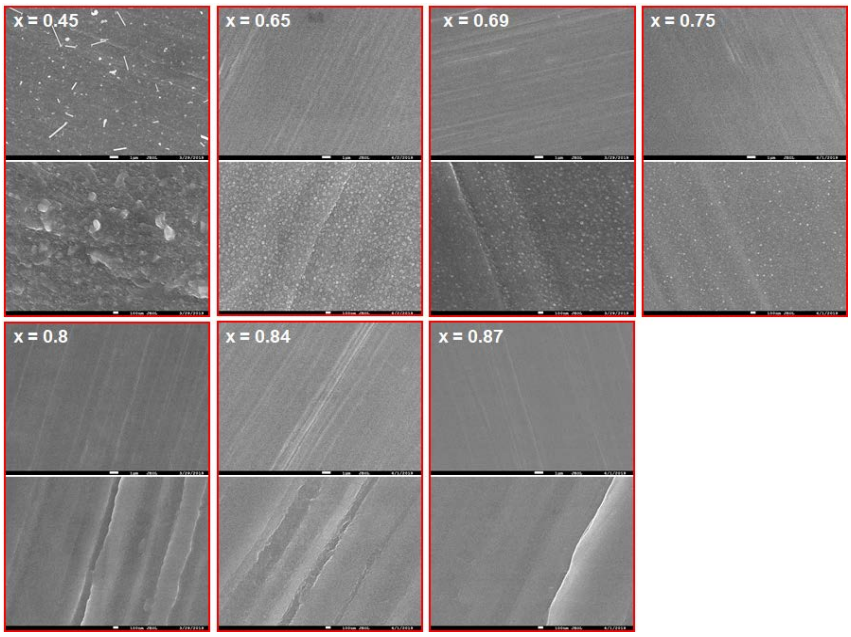

Figure 18. SEM images of co-sputtered Si-Sn films, x marks the content of Si. The upper and lower image in each panel is obtained at a low and high magnification, with a scale bar of 1 μm and 100 nm, respectively.

All the as-produced films are analyzed using SEM and EDS analysis to evaluate the morphology and compositions. The Si content increases from 0.45 to 0.87 in film #1 to #7. **Figure 18** shows the SEM images of all the co-sputtered Si-Sn films, the upper and lower image in each panel is obtained at a low and high magnification, with a scale bar of 1 μm and 100 nm, respectively. As shown in **Figure 18**, most films (#2 to #7)

exhibit the striated morphology originating from the Cu substrate when they are examined at a low magnification, except film #1 with 0.45 Si, which shows some rod-like features related to the crystalline Sn, as evidenced by X-ray diffraction (XRD) (see FY19 Q2 Report). Closer examination at a high magnification reveals the variation of morphology with compositions. For films with Si content lower than 0.75 (#1 to #4), aggregated particles are observed with increasing Sn content, although film #2-4 appears X-ray amorphous. With Si content increasing up to ≥0.8, no visible particles are observed, instead, uniform films are obtained with the morphology similar to

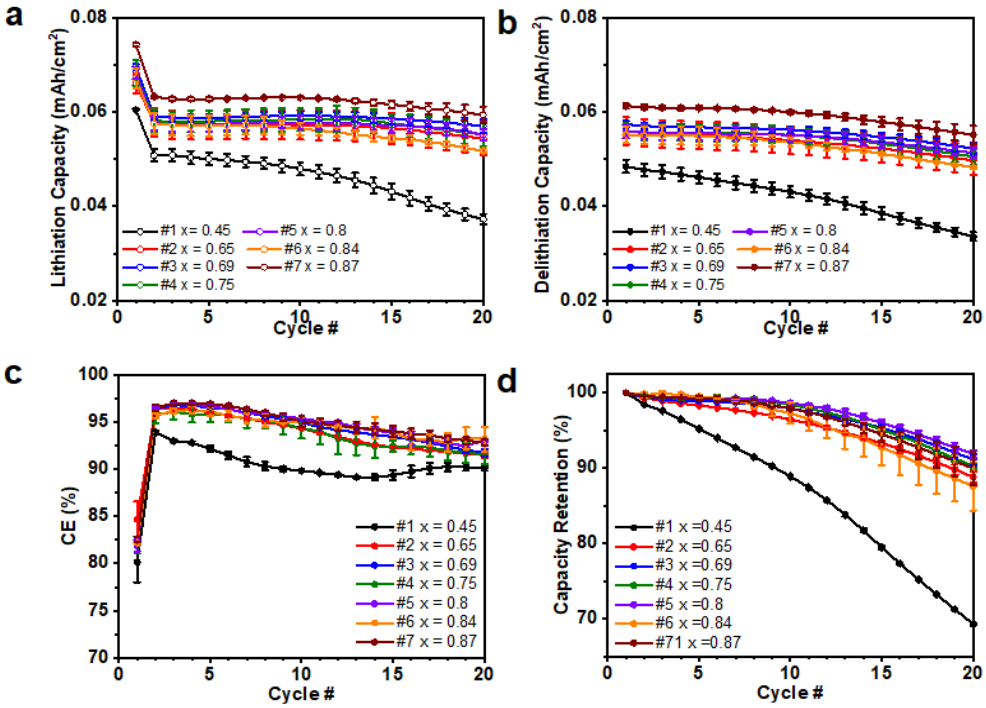

Figure 19. The electrochemical performance of co-sputtered Si-Sn films upon electrochemical cycling, x marks Si content. (a) Lithiation capacity, (b) delithiation capacity, (c) CE and (d) capacity retention.

the Cu substrate.

The initial lithiation and delithiation voltage profiles of these films were reported in the last quarter. The detailed electrochemical performance upon cycling is presented in **Figure 19**. Of all the films, film #1 with the Si content of 0.45 exhibits the distinctly sharp lithiation/delithiation peaks in the differential capacity plot, relating to crystalline Sn, which appear to diminish with decreasing Sn content. Film #5 and beyond, with the Si content ≥0.8, display almost complete features of amorphous phase (see FY19 Q2 Report). Because of the presence of crystalline Sn in film #1, as evidenced by both XRD and lithiation-delithiation profiles, this film shows poor capacity retention. As Si content increases, the other X-ray-amorphous films demonstrate dramatically improved cycling stability (>90 % after 20 cycles). From the combined physical and electrochemical characterization, the optimal Si content is determined to be around 0.8.

Conclusions

In this quarter, we studied the morphology and composition of the co-sputtered Si-Sn thin films using SEM and EDS, along with the detailed electrochemical performance upon cycling. Careful examination of the as-produced films further narrowed the formation range of amorphous films. The electrochemical characterization confirmed the amorphous films delivered much improved cycling stability. From the co-sputtering studies, we tuned the film compositions of varied stoichiometry and identified the optimal Si content in the Si-Sn composite films ranges around 0.8. The best performing Si-Sn film will be subjected to the SEI studies in the next quarter.

Effect of Electrode Capacity (n:p) Ratios on Electrochemical Performance (ANL)

M.-T.F. Rodrigues, S. E. Trask, D.P. Abraham

Background

The use of blended silicon-graphite (Si-Gr) negative electrodes increases the energy density of lithium-ion cells over those containing only graphite (Gr) electrodes. However, volume changes in the Si particles that occur during cycling causes deterioration of the solid-electrolyte interphase (SEI) layer on the particles resulting in further electrolyte reduction that immobilizes Li^+ ions and, therefore, capacity fade. Various approaches are being actively pursued to improve the performance of silicon-based negative electrodes, which include using

- optimally sized Si to prevent particle fracture and minimize reactions with the electrolyte,
- appropriate binders that allow electronic conduction while maintaining electrode integrity during cycling,
- electrolyte additives that enhance the stability of the silicon particle-electrolyte interface, which is continually disrupted during silicon expansion and contraction exposing fresh surfaces for solid electrolyte interphase (SEI) formation that trap additional lithium.

Another approach is to alter the electrode cycling windows by varying the negative (n) to positive (p) electrode capacity ratios. Our previous work has shown that the capacity fade rate of Si-based electrodes depends on the degree of lithiation/delithiation, which affects the expansion/contraction of the silicon particles. Limiting these volume changes can improve the longevity of Si-containing cells.

Figure 20 provides an explanation of the n:p capacity ratio concept. Shown in the **Figure** are half-cell electrode

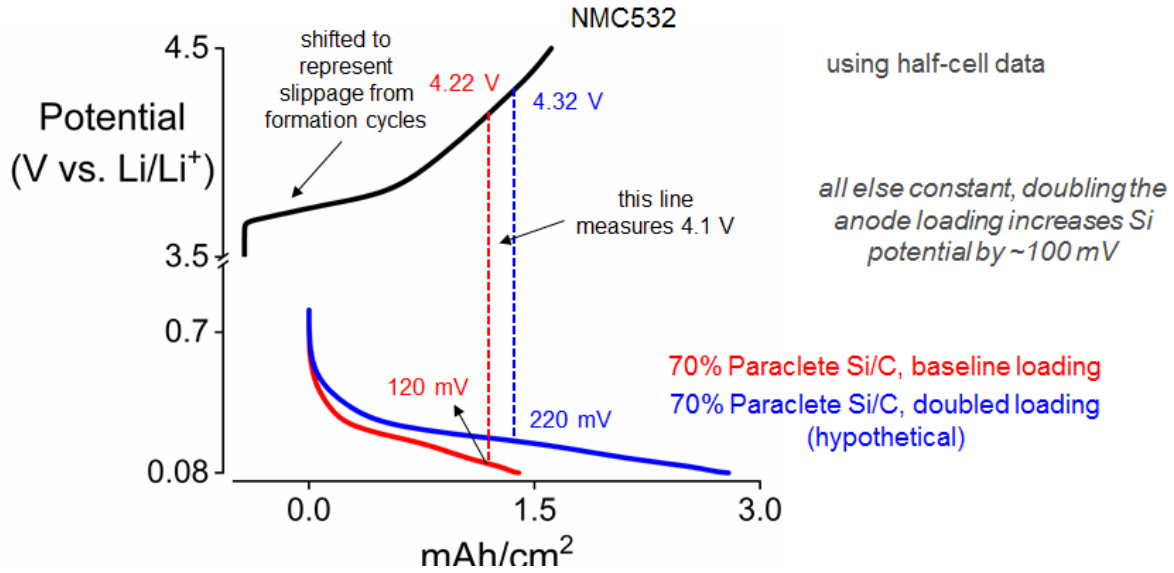

Figure 20. Explaining the concept. Schematic showing electrode potential vs. capacity plots for a NMC532 electrode (black) and two 70 wt% Si/C electrodes, one of which (blue) has twice the capacity of the other (red).

potential vs. capacity plots for our baseline NMC532 (black) and 70 wt% Si/C (red) electrodes; the curves are offset along the X-axis to account for the electrode potential shifts that occur during formation cycling. When a cell containing these electrodes is charged to 4.1 V, the positive and negative electrode potentials are 4.22 and 0.12 V vs. Li/Li^+ respectively. If we double the negative capacity by using thicker 70 wt% Si/C electrodes (blue) the positive and negative electrode potentials are 4.32 and 0.22 V vs. Li/Li^+ respectively at 4.1 V (cell voltage). The higher negative electrode potential would result in less Si expansion (and utilization) and thereby improve capacity retention. However, the higher Si content in the thicker electrode could result in greater electrolyte reduction, more solid electrode interphase (SEI) formation, and lower the initial capacity.

To examine the above concepts, we conducted tests on cells with various n:p ratios prepared by altering the thickness of the negative electrode. Both the NMC532 positive and Si negative electrodes were prepared at the CAMP facility; the latter contained the following constituents:

- 15 wt% Si, 73 wt% Graphite, 2 wt% C45, 10wt% LiPAA (henceforth referred to as 15Si)
  Coin cells with the above electrodes, Celgard 2325 separator, and the Gen2 electrolyte with 10 wt% FEC were assembled in an Ar atmosphere glove box and tested on a Maccor cycler using standard cycling protocols.

Results

The discharge capacity vs. cycle number plots for the various cells are shown in **Figure** 21: all capacities are listed as mAh/g-oxide, wherein the oxide refers to the weight of the NCM523 component in the positive electrode. The Coulombic efficiencies (CE) for cells with n:p ratios of 1.22, 2.18 and 2.82 were 76%, 70% and 67%; that is, the CE's did not decrease in proportion to the increasing n:p ratio. The initial capacities were also lower reflecting the decrease in the CE's. However, the capacities after 200 cycles were 20-25% greater for cells with the higher n:p ratios; i.e., the SEI losses in thicker electrodes are offset by the greater capacity retention, which results from lower volume changes in the Si particles.

Figure 21. Discharge capacity vs. cycle number for NCM523/15Si cells, with various n:p capacity ratios: 1.22 (black plot, our

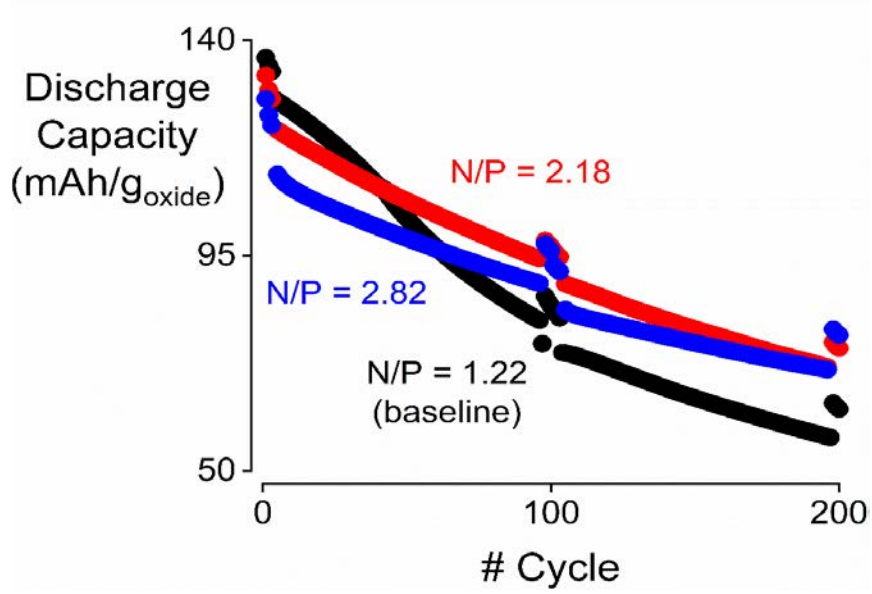

baseline), 2.18 (red plot) and 2.82 (blue plot), tested at 30°C. The test protocol contained two repetitions of 100 cycles. In each of these 100 cycles, cycles 1-3 are at a ~C/20 rate, 4-97 are at a ~C/3 rate and 98-100 are at a C/20 rate.

Conclusions

We compared the cycling behavior of NCM523/15Si cells with various n:p electrode capacity ratios. The highlights from our data are as follows:

- Initial capacity is greater for cells with a lower n:p ratio, reflecting less loss to the negative electrode SEI.
- Capacity after 200 cycles is greater for cells with a higher n:p ratio, reflecting the smaller volume changes that result from less lithiation of the Si particles in the thicker electrodes.
- Our data shows that an n:p ratio around 2.0 would improve capacity retention. Prelithiating the Si electrode to compensate for the initial loss to the SEI would further improve performance.

High Silicon Content Electrodes: CAMP Prototyping (ANL)

A.N. Jansen, S. Trask, B. Polzin, A. Dunlop, D. Kim

Background

Cycle life testing versus NMC532 was performed on the electrodes with electrochemically active carbon (hard carbon/SFG-6-L) at 23 wt.% combined with 60 wt.% Si, 2 wt.% C45 carbon additive, and 15 wt.% LiPAA binder that were developed in the second quarter. These electrodes were designed to operate with a 100 mV lithiation cutoff (vs. Li^+/Li). The full-cell performance of these two electrodes with 60 wt.% Si is shown in **Figure** 22, with a comparison to two previous full cells using 71 and 15 wt.% Si electrodes that used Mag-E3 graphite, C45 carbon, and LiPAA. It is encouraging to see that the Coulombic efficiency is improved for the electrodes with SFG-6-L flakey graphite and hard carbon. However, the capacity fade rate for the SFG-6-L flakey graphite is very similar to the 71 wt.% Si electrode. While the hard carbon electrode has a much lower fade rate, it suffered from a large irreversible capacity loss on the first cycle, which led to poor utilization of the cathode material.

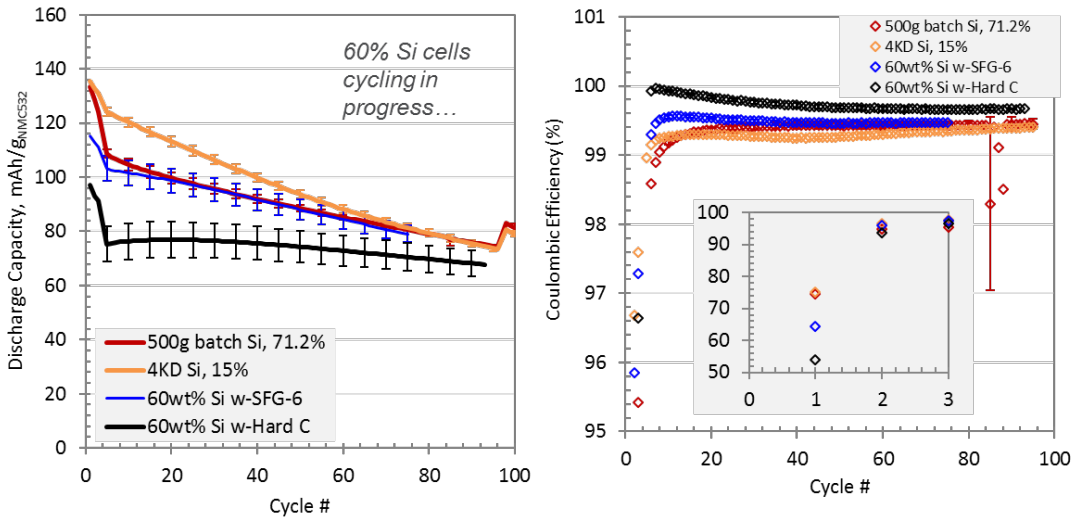

Figure 22. Cycle life data for NMC532 cathode versus 60 wt.% Si electrodes with 23 wt.% of either SFG-6-L flakey graphite or hard carbon. Comparison made to 71 and 15 wt.% silicon electrodes, all fabricated by the CAMP Facility. These cells were cycled between 3 to 4.1 V with the anodes balanced to 100 mV vs. Li^+/Li.

Collaboration with ORNL on the use of a Dispersant Process. The CAMP Facility is working closely with ORNL on their suggestion to use PAA as a dispersant in the silicon electrode slurry. Two slurries were tried with 1.8k PAA as the dispersant with either PAA as the binder, or LiPAA as the binder. Two more slurries were prepared without the dispersant to establish a baseline for this study. The PAA and LiPAA were 450k molecular weight. The compositions (dry wt. %) are as follows:

i. 80 / 10 / 9.5 / 0.5 [Si/C-45/450k PAA binder/1.8k PAA dispersant, water based]

ii. 80 / 10 / 10 [Si/C-45/450k PAA binder, water based]

iii. 80 / 10 / 9.5 / 0.5 [Si/C-45/450k LiPAA binder/1.8k PAA dispersant, water based]

iv. 80 / 10 / 10 [Si/C-45/450k LiPAA binder, water based]

The order of addition is a variable that is also being explored, which will be discussed in the future. The slurries above were mixed all at once in a planetary ball mill as a first trial. The rheology of the slurries was investigated and is shown in **Figure** 23 for the slurries based on LiPAA as the binder, with and without the PAA dispersant. Overall, the viscosity-shear rate behavior was very similar, with the dispersant lowering the viscosity slightly, as can be expected.

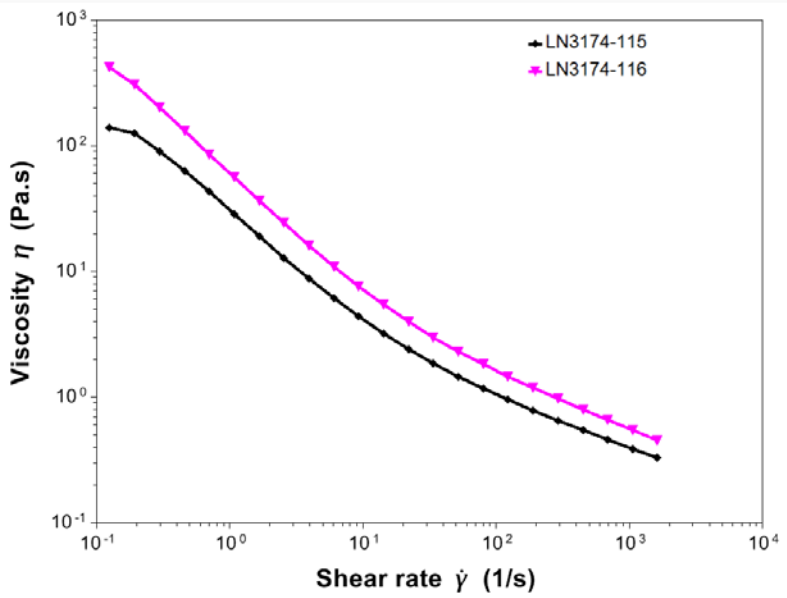

Figure 23. Viscosity vs. shear rate for 80 wt.% Si using LiPAA binder with PAA dispersant (LN3174-115) and without PAA dispersant (LN3174-116). Rheology measurement performed using a cone-plate geometry with a cone diameter of 20 mm and an angle of 2°. The temperature was held at 25 °C.

Some general comments can be made regarding the resulting electrode quality. The electrodes based on LiPAA were much more uniform than the electrodes based on PAA binder. The addition of the dispersant had a lesser impact on the electrode quality. Half cells were made with these four electrodes and initial tests are underway. Early results indicate that the cells with PAA as the binder have much better capacity utilization. These results will be confirmed and expanded in the next quarter.

Effort will continue to be directed to improving the slurry mixing and coating processes for these high Si electrodes. Some areas that are being explored are the molecular weight of the PAA binder (250k vs. 450k), the choice of solvent (water vs. NMP), and the order of addition/mixing. Additional efforts will be directed to exploring the impact of n:p ratio and cell voltage window. Collaborations will continue with ORNL for their guidance on incorporating dispersants in the slurry-making process to improve electrode homogeneity.

High Silicon Content Electrodes Stabilized with In-situ Coatings (ANL)

Baris Key, Binghong Han, Fulya Dogan, Chen Liao, Steven Trask, Jack Vaughey (ANL)

Background

The overall reactivity of lithium silicide Zintl phases that form upon lithiation of silicon greatly affects the formation and stability of the SEI and has been shown to reduce the efficiency of the Li-Si system. It is essential to control this reactivity by tuning the chemistry in order to achieve a stable high efficiency silicon anode electrochemistry.

Results

In the SEISta quarterly report we've demonstrated that Li-Mg-Si ternaries (or other M such as Zn, Al or Ca) to be chemically stable against common electrolyte solvents and they can be formed *in-situ* through electrochemical co-insertion after adding $Mg(TFSI)_2$ (or salts Zn, Al or Ca) of as the secondary salts into the electrolyte formulation in low concentrations.[1] We also show that the phenomenon fundamentally changes the traditional Li-Si binary chemistry while minimally effecting the electrochemical profiles, capacities and rate capabilities.[1] Li-Mg mixed salts stabilize the lithiated Si phases and reduce their side reactions with the electrolytes.[1] The half-cell electrochemical test results show higher capacities, superior cyclabilities, and improved Coulombic efficiencies with the new silicon electrolyte formulations containing $Mg(TFSI)_2$ as the secondary salts to $LiPF_6$ in comparison to the standard electrolyte.[1] In order to evaluate real-world battery performance against two standard baselines (Si+GenF and Graphite+Gen2), the new electrolyte formulations shown in Table 3 were tested in a full-cell configuration in coin cells using standard commercially relevant electrodes (electrode loading levels given in the experimental section) made in Argonne's CAMP Facility. Full cells were assembled using NMC532 ($LiNi_{0.5}Mn_{0.3}Co_{0.2}O_2$) or Li-rich HE5050 ($Li_{1.2}Ni_{0.2}Co_{0.2}Mn_{0.6}O_2$) cathodes countered by graphite-free Si anodes or traditional graphite anodes. The full-cell configurations were chosen based on the observations that neither M cation intercalates into graphite nor has an appreciable insertion chemistry related to the selected cathodes. The full-cell electrochemical performance is shown in **Figure** 24, and the representative voltage profiles are shown in reference 1. For the combination of NMC532 cathode + Si anode, when aggressively cycled between 3.0 V and 4.1 V at C/3 (with 4.1 V holds at the end of each charge cycle), using GenFM electrolyte can lead to a higher capacity retention rate of 68% over 90 cycles compared with that using baseline GenF electrolytes (49% over 90 cycles). Such improved capacity retention rate is still lower than the baseline graphite-anode result (96% over 90 cycles), but further developments in optimized and compatible binders and electrolyte formulations as well as new Si materials can certainly improve this performance further. Simply using Si anodes dramatically increases the specific total electrode weight capacity and energy density of the full-cell configuration, as shown in **Figure**s 24b and 24c. Adding a secondary Mg salt into the electrolyte brought an improvement of about 0.15% to the coulombic efficiency (see **Figure** 24d), which were over 99.3% although still lower than that of graphite-anode full cells (~99.5%). In addition, using Mg-Li mixed salts leads to lower initial impedance after the formation cycles as well as after 90 aging cycles, as shown in reference 1, which is likely caused by a more favorable SEI formation on Si electrodes with Mg co-insertion. Doubling the Mg concentration does not provide any obvious benefits to capacity or cyclability (see reference 1), suggesting enough Mg is provided for the co-insertion process. The fact that no negative response is detected with 0.2 M $Mg(TFSI)_2$, additional salt reservoir can be used to avoid depletion of the secondary salt due to extrusion or other reactions in certain long life applications. Another feature of the new chemistry is that the new formulations are fully compatible with graphitic anodes and can be used with graphite + silicon blends. As shown in reference 1, the full cells made by 15%Si+73%Graphite blended electrodes vs. NMC532 cathodes gain very similar performance improvements in the GenFM electrolyte, clearly demonstrating that the Mg salt is not impacting the electrochemistry at the graphite anode.

On the other hand, if Li-rich layered oxides (TODA HE5050 with 20% additional Li) were used with an increased voltage cutoff to 4.5V during the initial three C/20 formation cycles for the activation and the removal of extra Li,[2] the additional Li extracted from the cathode can be used to compensate the greater amount of Li consumption during the initial SEI formation on Si anodes, which is commonly referred as the 1st cycle irreversible capacity loss.[3] As a result of such intrinsic prelithiation, much higher capacities can be obtained by using the combination of Li-rich HE5050 cathode + Si anode when again cycled aggressively between 3 and 4.1 V using GenFM electrolyte, as shown in **Figure** 24e. Here the high-voltage cutoff of the formation cycles should be high enough that enough Li can be extracted to compensate the initial Li consumption, and at the same time not too high to cause the structural damage on cathodes or Li plating on the anode. In this paper, the high-voltage cutoff of the formation cycles was selected as 4.5 V because it can provide better electrochemical performance than the lower (4.1 V) or higher (4.7 V) cutoffs, as shown in reference 1. **Figure**s 24e-24g show that after adding Mg into the GenF electrolyte, the discharge capacities and energy densities of the HE5050+Si full cells increased by a dramatic ~30%, indicating that adding Mg secondary salt is an effective way to reduce the Li loss during the initial SEI formation with a more abundant Li source. Adding Mg salt also leads to lower initial impedance and slower impedance increase after 90 aging cycles, as shown in reference 1. The positive effect of intrinsic prelithiation can also be seen in unusually high initial coulombic efficiency values ~99.4% for silicon, approaching levels that can only be obtained with graphite-only anodes. **Figure** 24g shows the combined effect of using a Si electrode with GenFM electrolyte against a Li-rich electrode on the full cell electrochemical performance. The total active material weight specific energy density surpasses both graphite anode and silicon anode baselines by a remarkable 30% after 90 cycles. The cells tested above show stable extended cycling performance in **Figure** 25, with ~80 mAh/$g_{cathode}$ capacity after 270 cycles for cells with Li-rich cathodes (33% higher over baseline), and ~55 mAh/$g_{cathode}$ after 270 cycles for cells with NMC532 cathodes (120% higher over baseline). After 270 cycles, the Si electrodes in HE5050+Si full cells cycled in GenFM electrolyte show a bulk Si:Mg ratio of ~24:1, indicating there is still some Mg left inside of the Si particles after long cycling (see reference 1). Almost no Mg is detected in HE5050 cathode particles after 270 cycles (except for some potentially unwashed Mg salt left on the surface), indicating that Mg has little influence on the cathode. The dramatic increase in performance for lithium limited systems such as NMC532 cathodes and the compounded improvement in performance gained via use of mixed salts and intrinsic prelithiation clearly rationalize further improvements in capacities, cyclabilities, and efficiencies that can be obtained by optimizing other cell components such as binders and Si materials.[4]

Table 3. Formulations and notations of the electrolytes used in this study.

Notations	Components
Gen2	1.2 M $LiPF_6$ in 30 wt% EC + 70 wt% EMC
GenF	Gen2 electrolyte + 10 wt% FEC
GenFM	GenF electrolyte + 0.1 M $Mg(TFSI)_2$
GenFZ	GenF electrolyte + 0.1 M $Zn(TFSI)_2$
GenFA	GenF electrolyte + 0.1 M $Al(TFSI)_3$
GenFC	GenF electrolyte + 0.1 M $Ca(TFSI)_2$
GenFL	GenF electrolyte + 0.1 M LiTFSI

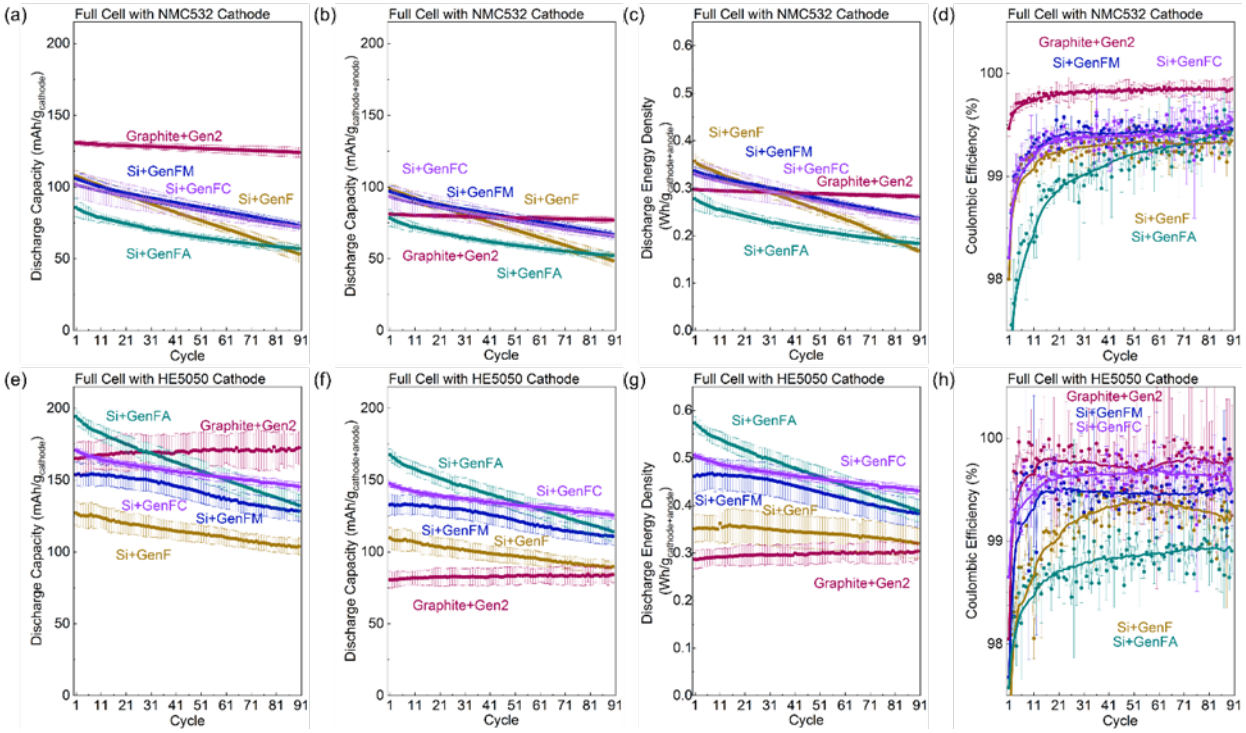

Figure 24. Full-cell electrochemical test results. Cells in panels (a)-(d) consist of NMC532 cathodes and Si or Graphite anodes (formation cycles are not shown). Cells in panels (e)-(h) consist of HE5050 cathodes and Si or graphite anodes (formation cycles are not shown). At the end of each charge step the cells were held at 4.1 V until the current dropped below C/50. The discharge capacities in panels (a) and (c) are normalized by the weights of cathode materials (NMC523 or HE5050). The discharge capacities and discharge energy densities in panels (b), (c), (f), and (g) are normalized by the total weights of cathode materials (NMC523 or HE5050) and anode materials (Si or graphite). Error bars represent the standard deviations of at least three measurements for each sample. Trend lines for the columbic efficiencies in (d) and (h) were calculated by a moving average of 15 adjacent points.

GenFA, GenFC, and GenFZ electrolytes shown in Table 1 with Al, Ca, and Zn salts were also tested in full-cell configurations. In the case of GenFZ electrolyte, the full cell loses all capacity promptly during the first formation cycle of the cycling protocol (data not shown), which is most likely due to the activity of Zn-ion in the cathode.[5] On the other hand, the Al- and Ca-salts like Mg work compatibly in the full-cell configuration. As shown in **Figure** 24, using Al-containing GenFA electrolyte leads to a lower coulombic efficiency compared with other electrolytes. When paired with NMC532 cathodes, GenFA leads to lower initial capacity but better capacity retention than the GenF baseline, which let it outperform the GenF electrolyte after ~80 cycles. When paired with HE5050 cathodes, GenFA shows the initial capacity even higher than GenFM but with a worse capacity retention, which might be due to its high capacity utilization or fast rising impedance. Extended cycles for GenFA show more decay in cyclability and performance when compared to GenFM (see **Figure** 25). It must be noted that despite the best efforts, GenFA electrolyte in pristine state had a yellow tint that could be due to impurities originating from the salt or indicative of some degradation, which may lead to the low stability and high impedance in GenFA electrolyte. Meanwhile, adding Ca salt into the electrolyte (i.e. using GenFC electrolyte) brings similar improved capacities, retention rates, coulombic efficiencies and impedance as in the GenFM electrolyte in NMC532-based full-cell tests, as shown in **Figure**s 1a-1d.[1] In HE5050-based full-cell tests, GenFC shows much higher capacities, better cyclability, higher efficiencies and lower impedance than GenFM (see **Figure**s 1e-1h),[1] indicating that the Ca-containing electrolyte performs better than the Mg-containing electrolyte with initial high-voltage activation process. These GenFC cells show a remarkable ~70% capacity retention after 270 cycles in extended full-cell tests as shown in **Figure** 25b.[1] The differences in electrochemical performance trends observed between GenFM, GenFA and GenFA can be due to a number of factors originating from the

complexity of the battery systems. In fact, both the cation and anion of the secondary salt can have effects in addition to the starting Si material, the binder and the solvent choices, which all influence the final electrochemical performance of silicon full cell. Therefore, more fundamental studies are critically required in the future for an in-depth understanding of the new chemistries demonstrated in this paper, which perhaps for the first time allow for an effective optimization of the full cell compositions with silicon anodes that can electrochemically outperform the well optimized graphite electrodes over the last few decades.

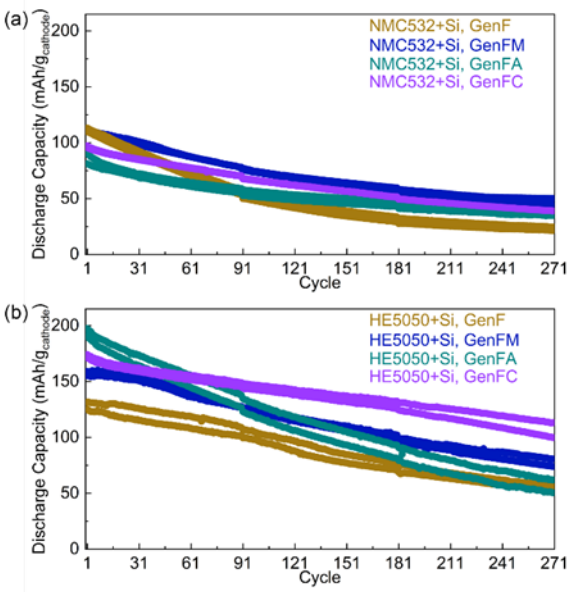

Figure 25. Discharge capacities of full cells using GenF, GenFM, GenFA, and GenFC electrolytes with extended cycles. (a) The full cells consist of NMC532+Si electrodes were cycled between 3.0 and 4.1 V at C/3 after three formations cycles between 3.0 and 4.1 V at C/20 (formation cycles are not shown). (b) The full cells consist of HE5050+Si electrodes were cycled between 3.0 and 4.1 V at C/3 after three formations cycles between 3.0 and 4.5 V at C/20 (formation cycles are not shown). At the end of each charging process during aging cycles the cells were held at 4.1 V until the current dropped below C/50. Two cells were tested for extended cycles on each cathode to show that the lifetime of the full cells are repeatable.

Conclusions

In this study, we show Li-M-Si ternaries to be chemically stable against common electrolyte solvents and they can be formed *in-situ* through electrochemical co-insertion after adding $M(TFSI)_x$ (M = Mg, Zn, Al, and Ca) as the secondary salts into the electrolyte formulation in low concentrations. Li-M mixed salts stabilize the lithiated Si phases and reduce their side reactions with the electrolytes. The electrochemical test results show higher capacities, superior cyclabilities, and improved coulombic efficiencies with the new silicon electrolyte formulations containing $Mg(TFSI)_2$, $Al(TFSI)_3$ or $Ca(TFSI)_2$ as the secondary salts to $LiPF_6$ in comparison to the standard electrolyte. The post-electrochemistry NMR, (HR)XRD, TEM and EDS characterizations demonstrate that adding Mg secondary salt promotes the doping of small concentrations up to 0.09 Mg per Si into silicon in the bulk during the lithiation process to form relatively more stable amorphous or semi-crystalline Li-M-Si ternaries, which fundamentally changes the traditional Li-Si binary chemistry while minimally effecting the electrochemical profiles, capacities and rate capabilities. Using Mg-containing electrolyte in NMC full cells improves the coulombic efficiencies by 0.15% and in turn the capacity retention rates by ~40% after 90 cycles. The impedance characteristics are also improved after adding the Mg second salt. We also show that Li-rich cathodes can be used effectively to couple with silicon electrodes for intrinsic prelithiation via the activation of the cathode at high voltages during formation cycles or even after extended cycling, which can dramatically increase the usable silicon capacities on top of the gains in coulombic efficiencies and retention rates, surpassing

full cell energy densities of cells coupled to graphite electrodes after 90 cycles. Extended-cycle tests show performance retention and Mg activity even after 270 cycles. Similar full-cell performance improvements can also be found via the addition of an Al or Ca salt into the electrolyte, however the Zn salt is found to be not suitable in full-cell configuration mainly due to the activity of Zn in the cathode. The results also suggest that a rich Zintl chemistry must be explored fundamentally further with this approach where other M cations, particularly the multivalents that can form Li-M-Si Zintl phases with minimum activity in the cell otherwise, can be incorporated via the electrolyte to provide *in situ* stabilization via the formation of Li-M-Si ternaries, Li-M-M'-Si quaternaries, or higher. The battery chemistry demonstrated in this study introduces a whole new and synergistic approach to stabilize silicon anodes and has the potential to be a fundamental building block in widespread application of Si anodes in lithium-ion batteries, particularly when used in conjunction with the advances in binder, electrolyte, and Si material developments as well as new prelithiation methods.

References

1. Han, B.; Liao, C.; Dogan, F.; Trask, S. E.; Lapidus, S. H.; Vaughey, J. T.; Key, B., Using Mixed Salt Electrolytes to Stabilize Silicon Anodes for Lithium-Ion Batteries via In situ Formation of Li-M-Si Ternaries (M=Mg, Zn, Al, Ca). *ACS Appl. Mater. Interfaces* **2019**.
2. Dogan, F.; Croy, J. R.; Balasubramanian, M.; Slater, M. D.; Iddir, H.; Johnson, C. S.; Vaughey, J. T.; Key, B., Solid State NMR Studies of Li_2MnO_3 and Li-Rich Cathode Materials: Proton Insertion, Local Structure, and Voltage Fade. *Journal of the Electrochemical Society* **2015,** *162* (1), A235-A243.
3. Dose, W. M.; Maroni, V. A.; Piernas-Muñoz, M. J.; Trask, S. E.; Bloom, I.; Johnson, C. S., Assessment of Li-Inventory in Cycled Si-Graphite Anodes Using $LiFePO_4$ as a Diagnostic Cathode. **2018,** *165* (10), A2389-A2396.
4. Obrovac, M. N.; Chevrier, V. L., Alloy Negative Electrodes for Li-Ion Batteries. *Chemical Reviews* **2014,** *114* (23), 11444-11502.
5. Pan, C.; Nuzzo, R. G.; Gewirth, A. A., $ZnAl_xCo_{2-x}O_4$ Spinels as Cathode Materials for Non-Aqueous Zn Batteries with an Open Circuit Voltage of ≤2 V. *Chemistry of Materials* **2017,** *29* (21), 9351-9359.

Publications

- Binghong Han, Maria Jose Piernas-Muñoz, Fulya Dogan, Joseph Kubal, Stephen E. Trask, Ira D. Bloom, John T. Vaughey, Baris Key "Probing the Reaction between PVDF and LiPAA vs Li7Si3: Investigation of Binder Stability for Si Anodes" J. Electrochem. Soc. **2019** volume 166(12), A2396-A2402; doi: 10.1149/2.0241912jes
- Han, B.; Liao, C.; Dogan, F.; Trask, S. E.; Lapidus, S. H.; Vaughey, J. T.; Key, B., Using Mixed Salt Electrolytes to Stabilize Silicon Anodes for Lithium-Ion Batteries via In situ Formation of Li-M-Si Ternaries (M=Mg, Zn, Al, Ca). ACS Appl. Mater. Interfaces **2019**.

Composite Silicon / Graphite Electrodes

Variable Temperature Performance of Silicon-based Composite Electrodes (ANL)

María José Piernas, Ira Bloom, Alison Dunlop, S. Trask, A. Jansen

Background

Silicon is considered as a promising anode material to replace graphite in Li-ion batteries for electric vehicle (EV) applications, given the high capacity and, hence, the high energy density of this material. However, one factor that hugely affects the battery performance and that should not be overlooked, especially considering its ultimate goal, is the temperature at which an EV operates. To the best of our knowledge, the effect that temperature has on the cyclability of silicon has not been studied in depth. In this project, we are exploring the effect of temperature on the electrochemical performance of silicon anodes. With this purpose, we studied two different material/electrolyte systems: silicon (Si) in Gen 2 (1.2 M $LiPF_6$ in EC: EMC, 3:7 wt%) electrolyte with and without 10 wt% of fluoroethylene carbonate (FEC).

Results

In the last report, we discussed the role of varying temperature and its effect on data obtained from Si-Gr half-cells cycled in Gen 2 electrolyte. In this quarter, we have focused on the results obtained from CAMP silicon cells and compared them when cycled in Gen 2 and Gen2+ 10 wt% FEC.

The role of temperature is a critical variable in the cycling of lithium-silicon cells. As temperature increases the kinetics of SEI formation are enhanced, the solubility of SEI components is increased, and cycle life is decreased. This decrease may be related to the kinetic enhancement of the known silicon side reactions consume lithium cations and electrons from the battery circuit. **Figure** x displays how the capacity of Silicon electrodes varies as

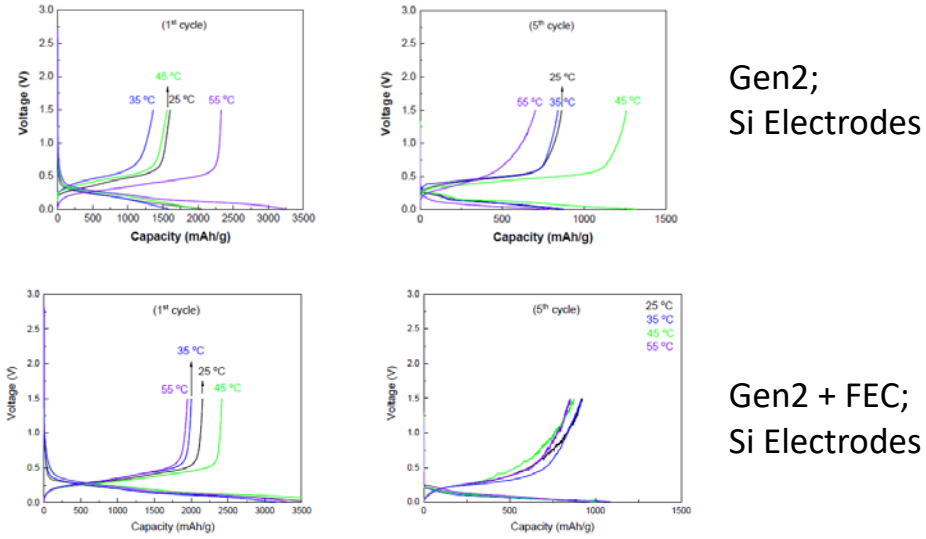

Figure 26. Charge and discharge capacity vs. cycle number plot of Silicon half-cells cycled at 25 (black), 35 (blue), 45 (green) and 55 ˚C (violet) containing Gen 2 electrolyte without FEC (a) and with 10 wt. % FEC (b). The filled and empty markers represent, respectively, the charge and discharge capacities. In all the cases, the Silicon electrodes were from CAMP (A-A017). Insets shows capacity obtained within the 5th cycle.

a function of cycle count and temperature applied. In absence of FEC, temperature affects the cyclability (**Fig. 26a**) of the material as well as its capacity (inset, **Fig. 26a**). The higher the cycling temperature, the larger the

capacity achieved. On cycling with and without FEC, the data for the 5th cycle is shown in **Figure** 26. In both cases the capacity after 5th cycle is diminished by about 50%, however the "spread' for the samples not cycled with an FEC additive is notably larger. In this no FEC added example the best capacity retention was noted for the sample cycled at 45 °C, while the 55 °C sample showed a dramatic drop in capacity. In comparison with addition of FEC, the "spread" was noted to be much tighter and have a cycling capacity less dependent on cycling temperature, although the capacity loss was approximately the same.

For the silicon-graphite cells reported previously and cycled under similar conditions, the role of FEC was found to be similar. In those evaluations, the samples cycled without FEC had higher "spreads" on 1st and 5th cycles than the cells cycled in the presence of an FEC additive, but the overall effect of FEC was not as notable when comparing the fade rates. This is consistent with the FEC mainly effecting the silicon-based electrochemistry (rather than the graphite) and as a minority component of the electrode its role may be less influential.

Conclusions

The electrochemical performance of Silicon half-cells has been evaluated versus temperature and with and without FEC. In similar studies from Si-Gr cells reported previously the role of temperature and FEC addition was found to be small (Coulombic efficiency). In this study 70% Si cells were evaluated and as predicted the role of FEC was found to much more notable in terms of Coulombic efficiency versus temperature.

Fracture Behavior with Polymer Binder Capping Materials (NREL)

Jaclyn Coyle, Yanli Yin, Chelsea Cates Nathan Neale (NREL)

Background

Using silicon nanomaterials is a widely accepted strategy for mitigating the extreme volume expansion associated with the lithiation of silicon and the accompanying capacity fade. However, the high surface area of silicon nanomaterials provides more opportunity for electrolyte decomposition which leads to high irreversible capacity loss and low Coulombic efficiency. Silicon microparticles are available in large scale at a low cost and offer an alternative with lower surface area that have been shown to have high initial Coulombic efficiency [1, 2]. However, to make silicon microparticles viable, the drastic volume change and high stress of these larger particles must be mitigated. The goal of this project is to develop a more thorough understanding of the initial lithiation mechanics of the silicon crystalline microparticles through model crystalline electrodes.
The results of this work provide important analysis targeted at the initial crack formation of silicon and how polymer capping layers affect the lithiation depth and cracking formation of crystalline silicon. These findings may be applied to create a viable capping layer to reduce cracking in larger, more economical, silicon particles.

Results

Last quarter, we found that the formation of <110>-oriented buckles—induced by the anisotropic lithiation in crystalline Si during the 1st lithiation—results in cracks propagated along the <110> direction in the buckled region during 1st delithiation. Surprisingly, as the delithiation proceeds, new cracks oriented along the <100> direction appear in the intact area where no geological deformation occurred during the previous lithiation. We discovered that the <100>-oriented cracking follows the linear elastic mechanism developed for multilayer structures. By using linear elastic fracture mechanics, we have investigated the formation mechanism of <100>-oriented cracking. The results imply that the <100>-oriented cracking behavior depends on the mechanical properties of the Si substrate and the amorphous Li_xSi layer[3].The next step for this study was to modify the mechanical properties of the top surface layer of the crystalline silicon substrates by adding a polymer capping layer and observe how these polymer layers affect the electrochemically induced fractures in crystalline silicon anodes through FIB SEM analysis. In this set of experiments, a 1 wt% methanol or n-methylpyrrolidone (NMP) solutions of polyvinylidene difluoride (PVDF), polyacrylic acid (PAA) and carboxymethylcellulose (CMC) were spin-coated onto native oxide (SiO_x)-terminated crystalline silicon substrates and lithiated to the same extent as an uncoated SiO_x-terminated silicon anode to directly compare crack formation under the same level of silicon lithiation. For lithiation, 10 μA cm^{-2} of current was applied to the working electrode for 60 h using 1.2 M $LiPF_6$ in EC/EMC = 3/7 (wt%) with 10 wt% FEC electrolyte. The same current density was applied for delithiation with a cutoff voltage of 1.5 V (*vs.* Li/Li^+). **Figure** 27 shows

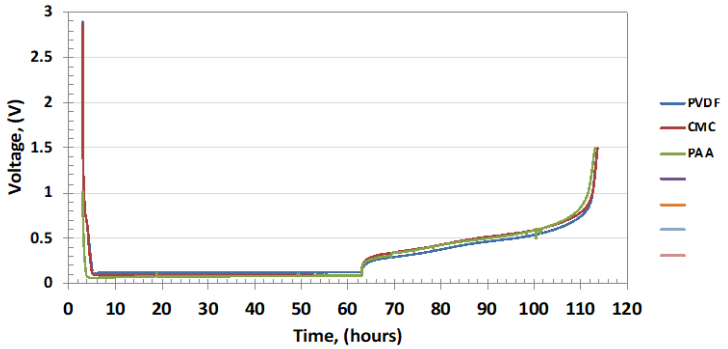

Figure 27. First cycle lithiation and delithiation at 10 uA/cm^2 for uncoated, PVDF-coated, CMC-coated and PAA-coated Si(100) wafer electrodes using 1M $LiPF_6$ in EC:EMC 3:7wt% solution with 10wt% FEC added

the electrochemical data for the PVDF-, CMC- and PAA-coated crystalline silicon substrate, with lithiation commencing ~3 h after applying current. Delithiation is slightly faster than lithiation, with the 1.5 V cutoff voltage achieved after 50 h.

In order to study the morphology of these crystalline silicon substrates with different polymer coatings, fast ion bombardment scanning electron microscopy (FIB SEM) images were taken of the surface of the cycled samples after rinsing in dimethylcarbonate (DMC) for 5 min. **Figure** 28 shows a summary for the FIB SEM images diplaying the crack formation for each of these anodes.

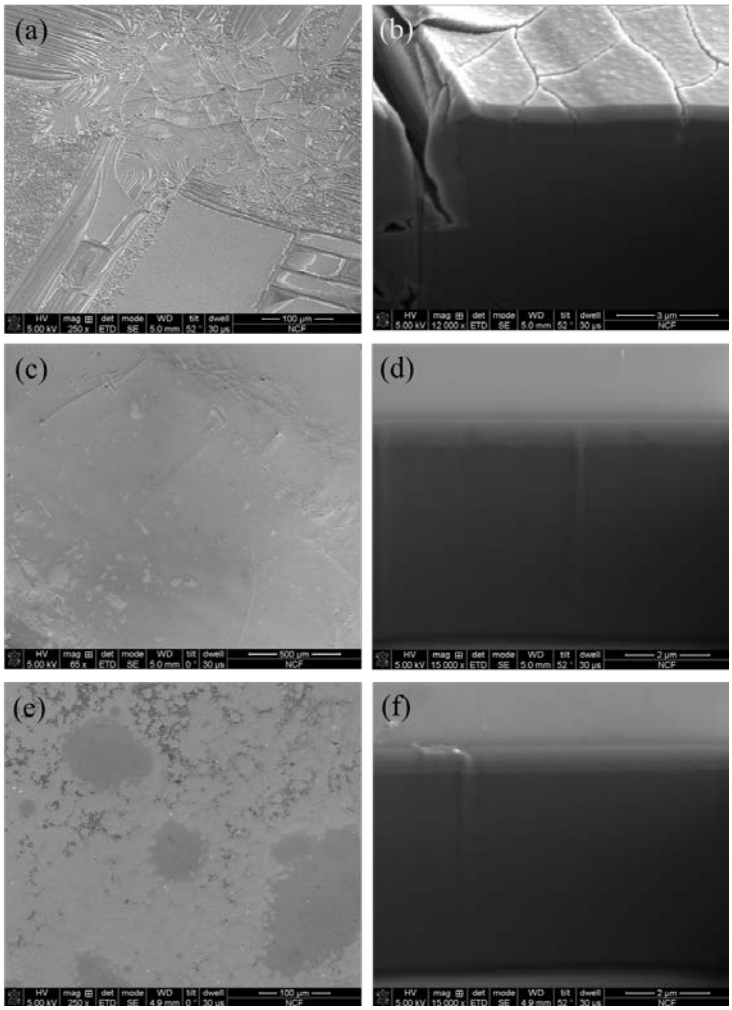

Figure 28. Morphologic study of the cracking behavior on the surface and with depth using FIB cross-section SEM images for (a,b) PVDF-coated, (c,d) CMC-coated and (e,f) PAA-coated crystalline silicon

A slow lithiation rate and long voltage hold was used in order to attempt to regulate the amount of lithium inserted into the top layer of the silicon substrate so that the stresses applied or mitigated by the polymer layers would be consistent. The capacity for each of these samples was approximately 0.2160 mAh and the amorphous surface layer formed during lithiation for all three polymer capping layers was approximately 600 nm deep (**Figure**s 2b,d,f) so we assume the surface stresses for each polymer sample are comparable. We found that PVDF-coated silicon behaves in a very similar way to uncoated silicon indicating that the mechanical behavior or strength of the bond to the silicon surface of the PVDF binder is not robust enough to mitigate the regular cracking formation of silicon. In contrast, we find that both PAA- and CMC-coated samples, no cracks were observed. It was also noted that for the same rinsing procedure the PVDF layer was completely removed while

the CMC and PAA both remain visible. This is another indication of the strength of their bonding to the silicon surface and/or poor solubility in carbonate solvent. This result suggests that PVDF binder may not be appropriate for Si-based electrodes, as it either does not bind strongly to the Si surface or dissolves in the electrolyte.

In Q4, we plan to continue similar experiments to quantify the effects of surface capping layers on mechanical stress and cracking behavior of silicon anodes with new PAA-based polymers developed by Lu Zhang (Argonne National Lab). Additionally, we are developing slurry ink formulations and will compare these new binders along with plasma-synthesized Si nanoparticles under air-free conditions to evaluate the performance of these new PAA-based binders initially in half-cell configuration. These studies will set up experiments to be conducted in FY20 on the performance of these new ANL binders with plasma-synthesized Si nanoparticles (NREL) or milled Si nanoparticles (ORNL) under air-free conditions in full cell configuration. This planned future work will complement studies by John Zhang (ANL) using water-based slurry formulations and allow comparison of these new binders under air-free vs. ambient environments.

Conclusions

In our previous work, we determined that the cracking mechanism of crystalline silicon substrates is heavily dependent on the mechanical properties of the surface layer and detailed a previously overlooked formation of <100>-oriented cracking. In this study, we used the application of three different polymer films as capping layers on the crystalline silicon substrate to emphasize how the mechanical properties as well as binding behavior of these surface layers also play a critical role in silicon crack formation.

References

1. Choi, S., et al., *Highly elastic binders integrating polyrotaxanes for silicon microparticle anodes in lithium ion batteries.* Science, 2017. **357**(6348): p. 279-283.

2. Munaoka, T., et al., *Ionically Conductive Self-Healing Binder for Low Cost Si Microparticles Anodes in Li-Ion Batteries.* Advanced Energy Materials, 2018. **8**(14): p. 1703138.

3. Yoon, T., et al., *Electrochemically induced fractures in crystalline silicon anodes.* Journal of Power Sources, 2019. **425**: p. 44-49.

Silicon Surface Functionalization (ANL)

John Zhang, Sisi Jiang (ANL)

Background

In this quarter, silicon electrode with 100% surface-functionalized SiNPs (pristine Si-H terminated SiNPs prepared by NREL) was fabricated and its electrochemical performance was evaluated in the anode half-cell and the full-cell. Furthermore, HF-etching treatment was successfully demonstrated on the commercially available SiNPs in order to obtain large quantity of Si-H terminated SiNPs as the new baseline active anode materials for the study.

Results

Figures 29a-29d shows the electrochemical performance of the SF-SiNPs in half and full cell. Due to the high reactivity of Si-H group, the pristine Si-H terminated SiNPs showed a very low capacity and Coulombic efficiency. In contrast, after surface functionalization, both initial capacity, the Coulombic efficiency and the cycling stability are significantly improved as shown in **Figure 29a, 29b** and **29c**, respectively. Further, when this new anode was paired with a NMC532 cathode, the cell showed an initial charge capacity of 136 mAh/g with a Coulombic efficiency of 80.8% at C/20 rate. A capacity retention of 89% was obtained for 100 cycles when cycled with a C/3 rate (**Figure 29d**), indicating the improved interfacial stability at the anode side after functionalization.

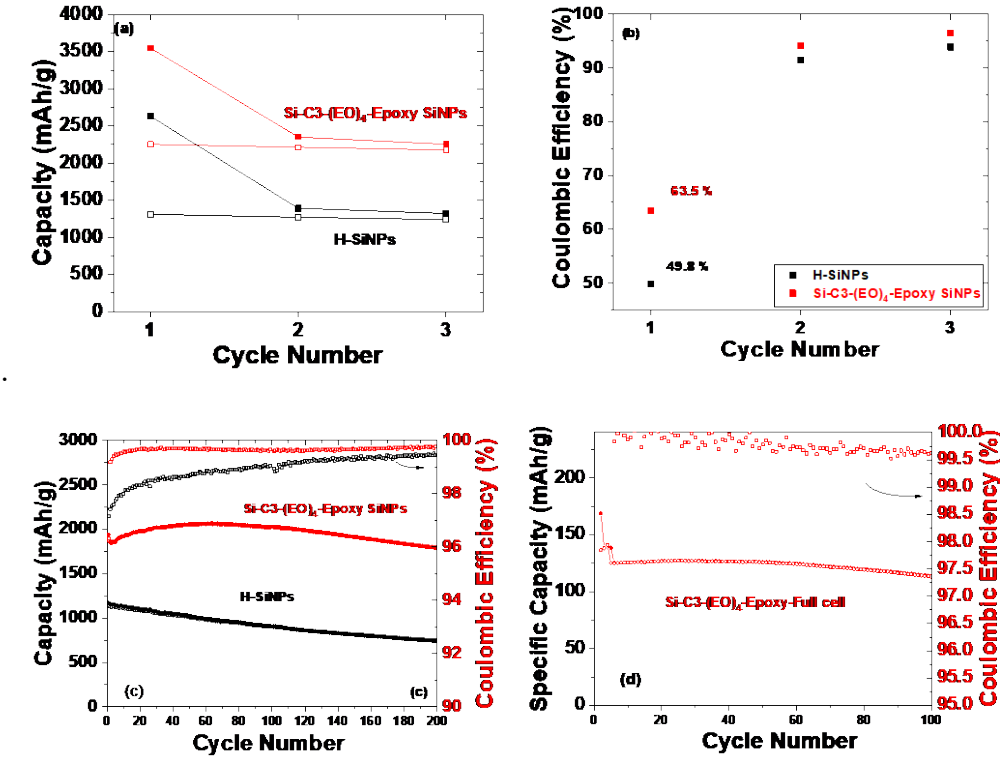

Figure 29. (a) Delithiation capacity and (b) Coulombic efficiency of Li/Si cells for three C/20 formation cycles; (c) capacity retention and Coulombic efficiency of Li/Si cells with C/3 rate, and (d) NMC532/Si full cell cycling stability. (Electrolyte: Gen 2+10 wt% FEC; Li/Si cell cutoff voltage 0.01 – 1.5 V, NMC532/Si full cell cutoff voltage 4.2-2.7 V)

Progress was also made for the HF-treatment on the Alfa Aesar SiNPs with an averaged particle size of 50 nm (*SiAA-50nm).* **Figure 30a** showed the IR analysis of the SiNPs before and after HF treatment. Si-O_x, Si-H and OSi-H stretching vibration were shown on the FT-IR spectrum of the pristine SiNPs. After HF-treatment, the intensity of Si-H peak increased with the decreasing intensity of O-SiH peak. The new peak corresponding to C-H bonds at wavenumber less than 3000 cm^{-1} is believed to be originated from the pristine particles. The Si-H SiNPs were then functionalized using a carbonate-containing functional group via a Pt-catalyzed hydrosilylation reaction (**Scheme 1**). The successful functionalization was confirmed by the disappearance of Si-H peak at 2100 cm^{-1} and the appearance of the characteristic peak (1725 cm^{-1}) of carbonyl group in the FT-IR spectra (**Figure 30b**). The electrochemical performance of SF-SiNPs was evaluated in half-cell. The carbonate-functionalized electrode showed a significant improvement in both initial capacity (**Figure 30c**) and Coulombic efficiency (**Figure 30d**) for the formation cycles. The cycling performance is on-going and will be reported in the next quarter.

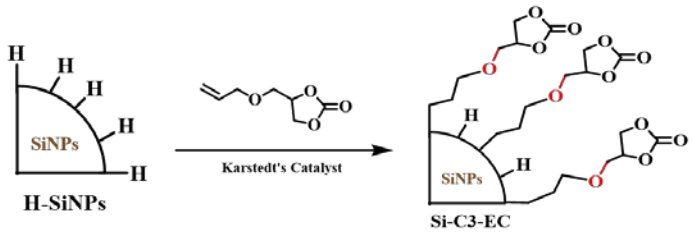

Scheme 1. Surface functionalization of H-terminated *SiAA-50nm* with ethylene carbonate-containing group.

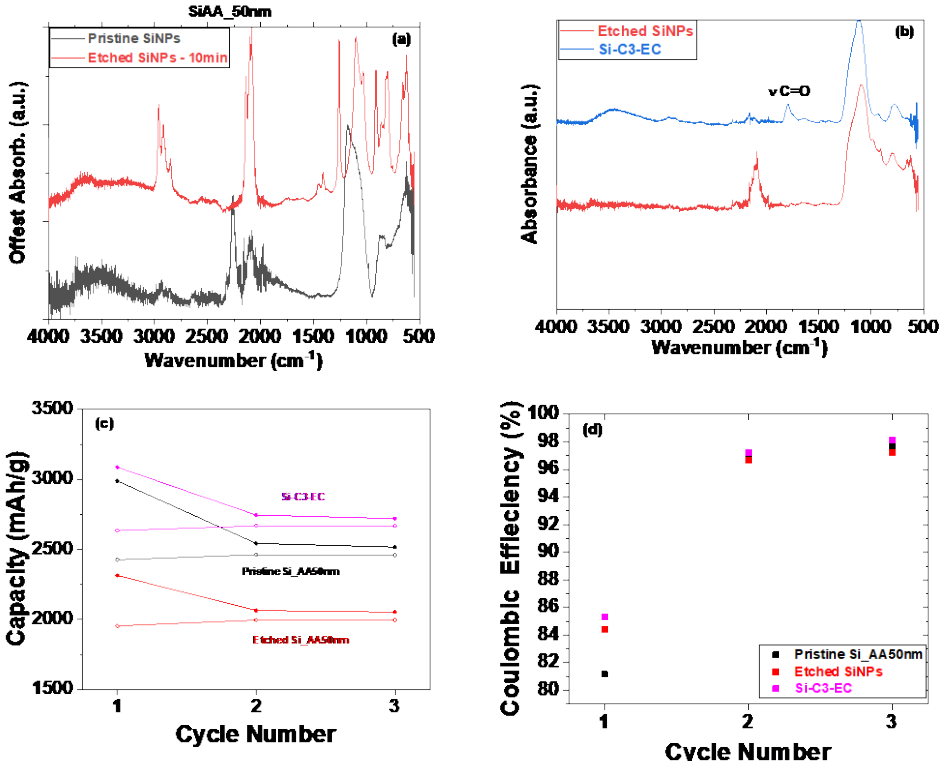

Figure 30. (a) FTIR spectra of *SiAA-50nm* before and after HF-treatment (the particle size provided here are vendor-claimed size), (b) after surface functionalization with a carbonate-containing group, (c) capacity and (d) Coulombic efficiency of Li/Si cells using pristine *SiAA_50nm*, H-terminated *SiAA_50nm* and Si-C3-EC SiNPs as active materials, respectively. (Electrolyte: Gen 2+10 wt% FEC; cutoff voltage 0.01 – 1.5V).

Conclusion

HF etching of various commercial silicon samples was attempted as a method to increase our supply of a hydride terminated silicon NP as the starting point of our surface functionalization studies. Various treatments were noted to cause differences in the recovered silicon materials, most notably the appearance of organic species and the decrease in silica content. Among the four commercial SiNPs sample, SiHQ_80nm and SiAA_50nm samples provided the most reproducible and clean H-terminated surfaces by HF etching. The surface functionalization of these two samples will be evaluated in the next quarter as our hydride silicon source.

Silicon Pre-lithiation Studies (Argonne National Laboratory)

Wenquan Lu, Yan Qin, Linghong Zhang, Christopher Johnson (ANL)

Background

One of the challenges to attaining a viable Silicon-based electrode in a working lithium-ion (LIB) cell is low first cycle Coulombic efficiency. To address the problem, prelithiation reagents have been investigated as a physical method to offset the losses that occur due to SEI formation, surface area expansion, and lithium or electron consuming side reactions. As an advantage they can be added to either the anode or the cathode. A prelithiation reagent provides extra lithium during the first formation cycle, therefore compensating the lithium loss caused by the irreversible reactions. A potential prelithiation material, Li_5FeO_4 has been synthesized by the Johnson group at Argonne and investigated as a cathode prelithiation reagent. Li_5FeO_4 (LFO) possesses a theoretical capacity of 867 mAh/g and potentially can release up to 5 lithium ions per mole to the cell upon the first charge via reaction.

In this work, we demonstrate the use of LFO in addressing the irreversible capacity loss of a silicon monoxide (SiO) – based electrode. LFO was mixed with $LiNi_{0.5}Co_{0.2}Mn_{0.3}O_2$ (NCM523) cathode materials. The resulting cathode was then paired with an SiO anode and the impact of LFO addition on the electrochemical performance of the cell was analyzed.

Results

The amount of LFO needed to compensate the Li loss of SiO is calculated to be approximately 10% of the NCM523 weight based on the first cycle voltage profiles. **Figure** 31 compares the two scenarios of full cell matching considering an N:P ratio of 1. **Figure** 1a shows the scenario when a SiO anode is paired with an NCM523 cathode. The experimental voltage profiles of the SiO half cell and the NCM523 half cell are used. Due to the difference in the first cycle coulombic efficiency and therefore the initial capacity loss, a significant portion of lithium extracted from the NCM523 cathode is used towards parasitic reactions in the SiO anode, as marked in **Figure** 31a. The loss of lithium in irreversible parasitic reactions leads to low Li utilization in the reversible cycling and therefore lower capacity of the cell. **Figure** 1b shows the scenario when a SiO anode is paired with an NCM523-LFO blend cathode. The LFO gives out lithium via irreversible reactions in the first charge, effectively providing the extra Li that is consumed by the parasitic reactions at the first charge of the SiO

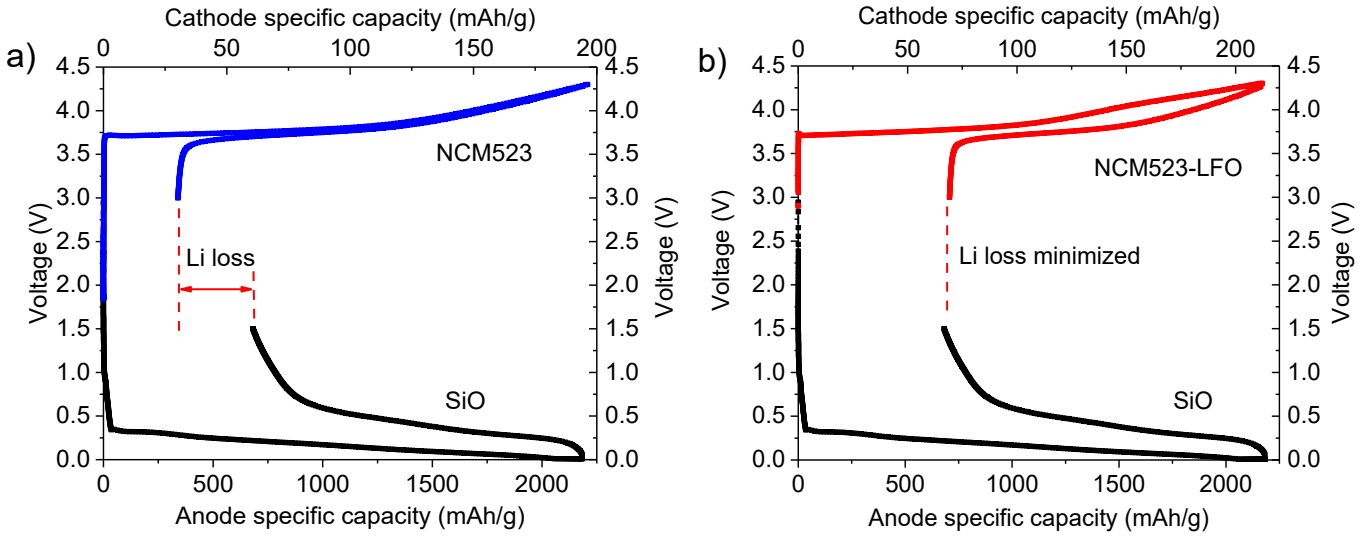

Figure 31 Full cell matching for SiO/NCM523 and SiO/NCM523-LFO

anode. A close to full utilization of lithium from the NCM523 cathode can be realized.

To test the impact of LFO on the electrochemical performance of the full cells, SiO anodes were paired with NCM523 cathode and NCM523-LFO blend cathode respectively for electrochemical performance evaluation. The corresponding full cells were cycled for three formation cycles between 2.5 V and 4.3 V at C/10 rate first, followed by 50 cycles of cycle test at a charge rate of C/5 and a discharge rate of C/3. A C/10 cycle was also performed at every 10th cycle during the cycle test. **Figure** 4 compares the first cycle voltage profiles and cycle performance of SiO/NCM523 and SiO/NCM523-LFO full cells. The specific capacity of SiO/NCM523-LFO full cells shown in **Figure** 4 is based on the weight of NCM523-LFO blend.

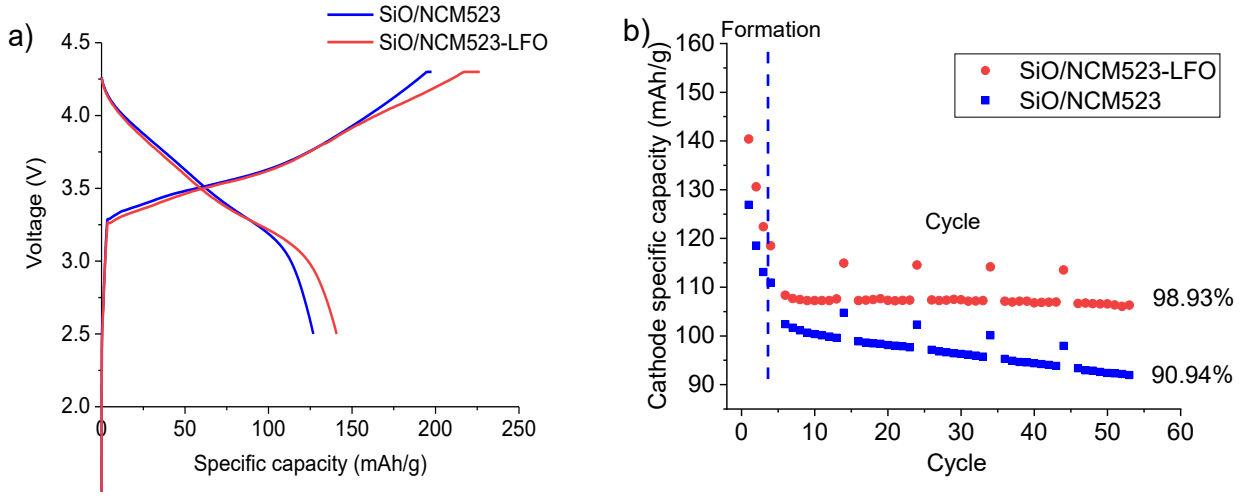

Figure 32 a) voltage profile comparison and b) cycle performance comparison of NCM523/SiO and NCM523-LFO/SiO. The capacity of SiO/NCM523-LFO full cells are calculated based on the total weight of NCM523-LFO blend

As shown in **Figure** 32a, comparative to SiO/NCM523, SiO/NCM523-LFO shows an increased first cycle charge and discharge capacity. Specifically, the discharge capacity increased from 126.8 mAh/g for SiO/NCM523 to 140.8 mAh/g for SiO/NCM523-LFO based on the weight of NCM523/LFO blend, or 154.9 mAh/g based on the weight of NCM523 alone. The LFO addition leads to a significant 22% more lithium utilization from NCM523, and an 11% improvement in the discharge capacity of the cell. **Figure** 32b compares the complete electrochemical performance for SiO/NCM523 and SiO/NCM523-LFO full cells. Fast capacity fade in the initial three formation cycles was observed for both SiO/NCM523 and SiO/NCM523-LFO. The fast capacity fade of SiO electrodes in the initial cycles has been reported in our previous work and was attributed to the capacity loss from incomplete delithiation of SiO due to large volume change during cycling. As the SiO anode stabilizes, the capacity retention of the cells improve. During the cycle test, SiO/NCM523 showed a capacity retention of 90.94% for 50 cycles, while the addition of LFO improved the capacity retention to 98.93% for 50 cycles. Furthermore, the reversible capacity was improved from 102.4 mAh/g for SiO/NCM523 to 119.7 mAh/g for SiO/NCM523-LFO at the start of the cycle test, or 16.9% improvement in lithium utilization from NCM523.

Conclusions

To conclude, in this work we have demonstrated the use of Li_5FeO_4 (LFO) to compensate the initial capacity loss of silicon monoxide (SiO). The resulting full cell showed a 22% improvement in the lithium utilization of the NCM523 cathode active material, or 11% improvement capacity improvement based on the NCM523-LFO blend. An improvement of capacity retention from 90.94% to 98.93% in the 50 cycles of cycle test was also improved.

Lithium Inventory & Soluble SEI Species (Argonne National Laboratory)

Nasim Azimi, Zhangxing Shi, Lu Zhang, Gabriel Veith (ORNL), Christopher Johnson

Background

This project has been continued by studying the SEI formation using a rotating ring disk electrode (RRDE) design rotating unit with bi-potentiostat located in the Ar glovebox. A study of the trapping of lithium in the SEI and the electron transfer and stability of the SEI will be conducted. The following are the objectives moving forward.

(1) Measure by-products from electrochemical/chemical reactions that occur.
(2) Determine the location of the electron transfer event during (de)lithiation: for example, at the exterior of the SEI, interior of SEI, or the interface of SEI/Si buried surface.
(3) Studying any redox active products at the ring electrode coming of the material at the disk where the rotation speed will also allow us to probe the kinetics of the reactions.
(4) Study the nature of the silicon surface effect which can greatly affect the composition and thickness of the SEI layer.

Results

We received a number of 50 nm sputtered Si thin films on the Cu disk RRDE tip electrode from Dr. Veith (ORNL). Unfortunately the adhesion of the films onto the Cu substrate was not satisfactory in order to successfully accomplish the electrochemical rotating voltammetry in the flooded RRDE cell (also electrode is inverted which is problematic (fighting gravity)). Thus, instead, we prepared a drop-coated/cast electrode from a slurry of 70% Paraclete Si, 20% PAA binder and 10% C45 carbon black. The slurry was then coated on the surface of Cu disks and dried for 12 hours at 80 ^{o}C in vacuum oven. Fig1 a-d shows the first sweep rotating ring disk voltammetry results on two of these electrodes (a. Si (70%) electrode as the disk, b. Si(70%) as the disk) and Pt for ring electrode (c. Pt ring, d. Pt ring, e. Pt ring) and Li foil was used as reference and counter electrode. The difference between (a.) versus (b.) and (c.) versus (d.) is the addition of FEC additive (10%). In the experiment, the RRDE was rotated at 500RPM in 150 mL of electrolyte in order to sweep away any products from the disk to be subsequently electrochemically oxidized or reduced at the Pt ring electrode. The disk and the ring voltage were simultaneously swept at 2 mV/s from OCV of 3.0 V reductively down to 0.01 V vs. Li/Li^{+} and oxidatively back up to the stopping voltage of 3 V.

Fig33 a and b shows the first sweep i-v curves for the Si (70%) disk electrodes in GEN2 (a.) and Gen2 + 10% FEC (c.) electrolytes. In (a.), there is a reductive peak at E=1.42V, which can be assigned to the formation of SEI on the Si electrode. Slightly thereafter, the Pt ring electrode picks up a reductive species at slightly lower voltage of E=1.1V likely formed as a result of some electrochemically active species given off after SEI formation at the Si disk. These processes may be linked together. Note that we plan to conduct the same experiment with Cu metal as the ring (to distinguish between any Li-Pt alloying reactions). There are also a set of three oxidations that occur at the Pt ring during the oxidative sweep at E=1.05V, 1.45V, and 1.8V.

Now when FEC is added to Gen 2 electrolyte (Fig33. c. and d.), the i-v curves are quite different both at the disk (c.), and the Pt ring (d.). In (c.), the FEC is clearly reduced at E=1.3V. Note the Si (de)lithiation current magnitude/shape is slightly different now itself due to different mass loadings of the drop cast Si (70%) disk electrode. The SEI peak seen in (a.) at E=1.42V is now obscured in (c.) by the FEC reduction. For the Pt ring electrode (d. trace), there is a large peak now present at a voltage of about 2.3 to 2.5 V vs. the Li reference electrode. This sharp reductive peak is also still present in FEC additive electrolyte even if the Li CE/RE electrode is replaced with an Ag/AgCl (RE) and Pt wire (CE) auxiliary electrodes. In Fig. 1 e. we plot b. and d. together on one graph, in order to accentuate the presence of this irreversible 2.5 V peak. Furthermore **Figure** 34 shows clearly that FEC passivates the Si (70%) electrode such that the current in the region of 1.5 to 10 mV

(light blue dash line) at the Pt ring detection electrode is quite diminished vs. non-FEC curve (light red dash line). The oxidation of product in the e. comparative plot also show that the oxidation peaks are eliminated.

The 2.5 V irreversible peak produced by the addition of FEC is unknown presently and we are continuing investigation of it with different electrolyte formulations and electrode WE materials.

a)

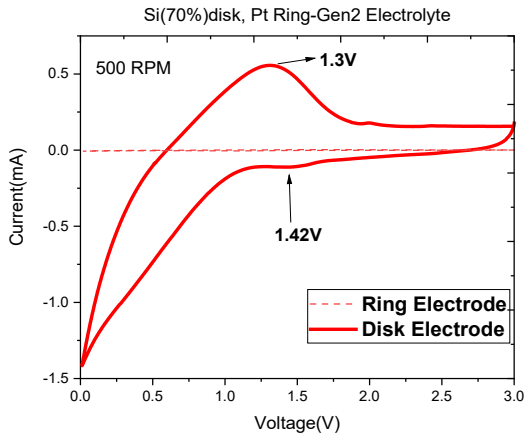

c)

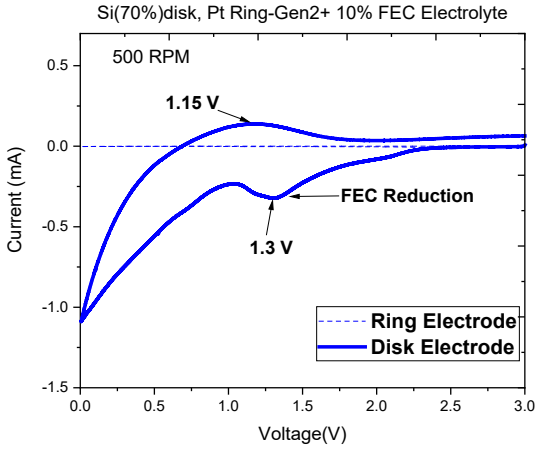

b)

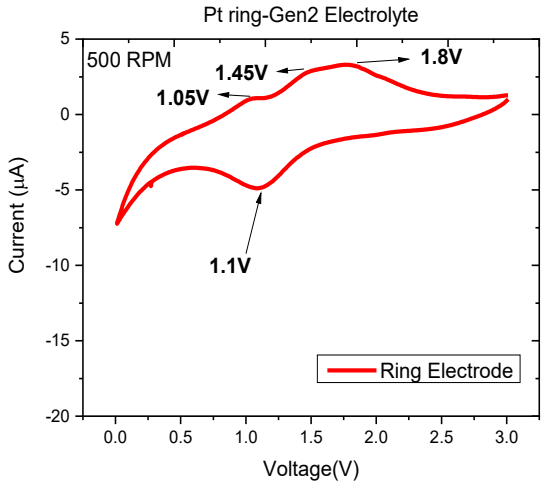

d)

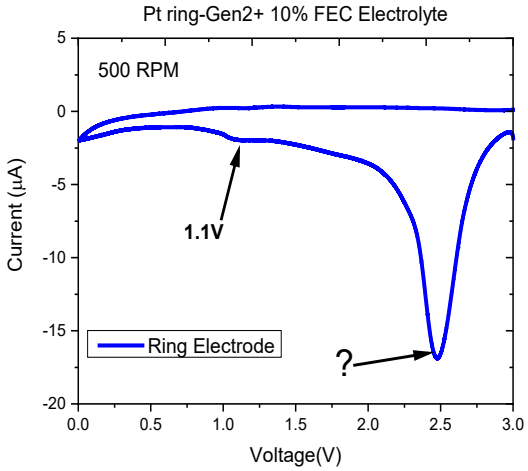

Figure 33. Rotating Ring Disk Electrode (RRDE) Voltammetry results shown for the first cycle with Si (70%) disk and Pt ring electrode with a,b) Gen2 and c,d) Gen2+ 10% FEC electrolyte with 2mV/s sweep rate and 500RPM rotation rate.

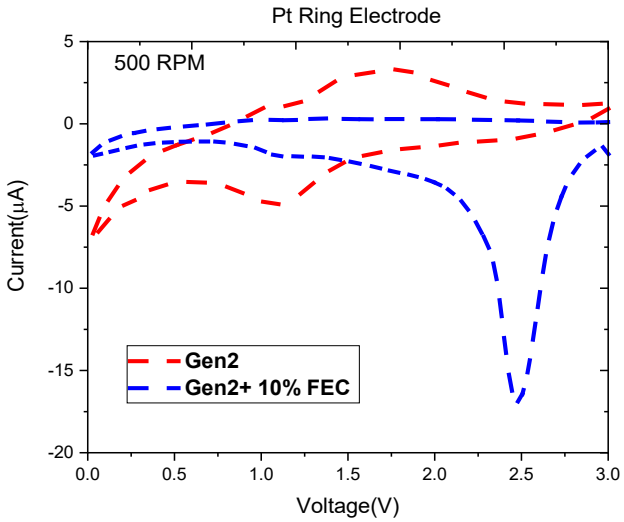

Figure 34 the effect of FEC detected on the ring electrode.

Conclusions

The set-up of the RRDE in the glovebox is operational and data is emerging. It is clear that measurable redox active species are coming off of the 70% Si drop-cast electrode at SEI formation and during simultaneous sweep at the Pt ring electrode. Addition of FEC mutes these peaks suggesting classic pre-passivation of the Si SEI. In addition, in many experiments we see a substantial irreversible reduction peak in our system at about 2.3 to 2.5 V vs. Li metal/Li CE electrode upon the addition of FEC. We hypothesize that there may be some impurity or trace water in the FEC additive. How that impurity or water affects the Si SEI is unknown. We are working on measuring its relative concentration by simple peak integration. For future work we will be focusing more on the SEI formation using the RRDE method with different Si surfaces and also additives that have proven to be efficient in improving the stability of the SEI layer.

Publications

- W. M. Dose, J. Blauwkamp, M. J. Piernas-Munoz, I. Bloom, X. Rui, R. F. Klie, P. Senguttuvan, C. S. Johnson, ACS Applied Energy Materials, 2019, 2, 5019-5028